ISSN 2096-7071 (Print)
ISSN 2097-3101 (Online)
CN 10-1629/R1

CHINA CDC WEEKLY

Vol. 8 No. 38 Sept. 18, 2026

中国疾病预防控制中心周报(英文)

BIRTH DEFECTS PREVENTION DAY ISSUE

Vital Surveillances

Evaluation of Perinatal Prevalence, Geographic Disparities, and Survival of Neural Tube Defects — China, 2006–2024 1167

Preplanned Studies

Shifting Burden of Neural Tube Defects from Early-Life Mortality to an Aging Population Living with Disability — China, 1990–2023 1174

Associations Between Longitudinal Antenatal Hematological Indicators and Risk of Patent Ductus Arteriosus in Newborns — Beijing, China, 2011–2025 1180

School-Based Scoliosis Screening Among Children and Adolescents — Wusu City, Xinjiang Uygur Autonomous Region, China, January 2026 1188

ISSN 2096-7071

China CDC Weekly

Editorial Board

Honorary Editor-in-Chief Hongbing Shen

Founding Editor-in-Chief George F. Gao

Advisory Board Member Jianguo Xu Liming Li Yu Wang Gabriel M Leung Zijian Feng

Editor-in-Chief Jianwei Wang

Deputy Editor-in-Chief

Zhuo Chen (USA) Zhibin Hu Qun Li Zhengliang Li Xiaoming Shi Yan Sun
Changjun Wang Tangchun Wu Yongning Wu Ningshao Xia Chihong Zhao

Editorial Board Member

Jianping Cao	Guobing Chen	Xi Chen (USA)	Gong Cheng	Gangqiang Ding
Xiaoping Dong	Pei Gao	Xin Guo	Jun Han	Mengjie Han
Weidong Hao	Na He	Yuping He	Guoqing Hu	Cunrui Huang
John S. Ji (USA)	Na Jia	Weihua Jia	Zhongwei Jia	Biao Kan
Haidong Kan	Jianqiang Lai	Lance Rodewald (USA)	Ni Li	Shizhu Li
Ying Li	Zhenjun Li	Zhongjie Li	Geyu Liang	Yuan Lin
Aidong Liu	Min Liu	Qiyong Liu	Qingjie Liu	Yawen Liu
Jinxing Lu	Xiangfeng Lu	David LYE Chien Boon (Singapore)		Fan Lyu
Jun Lyu	Huilai Ma	Jiaqi Ma	Chen Mao	Xiaoping Miao
An Pan	Jie Pan	Lili Ren	Guoqing Shi	Yuelong Shu
Chengye Sun	Quanfu Sun	Xin Sun	Hua Wang	Huaqing Wang
Hui Wang	Jianming Wang	Junling Wang	Lin Wang	Tong Wang
Shenghui Wu (USA)	Min Xia	Lin Xiao	Dongqun Xu	Hongyan Yao
Guojing Yang	Zundong Yin	Dianke Yu	Hongjie Yu	Siyan Zhan
Jianzhong Zhang	Jun Zhang	Liubo Zhang	Tao Zhang	Yanping Zhang
Wei Zhao	Yanlin Zhao	Maigeng Zhou	Xiaonong Zhou	Yongqun Zhu
Guihua Zhuang				

Editorial Office

Directing Editor Chihong Zhao

Managing Editor Yu Chen

Senior Scientific Editors

Xuejun Ma Daxin Ni Ning Wang Wenwu Yin Shicheng Yu Jianzhong Zhang Qian Zhu

Scientific Editors

Weihong Chen	Jie Dong	Tao Jiang	Dongmin Li	Xudong Li	Nankun Liu
Liwei Shi	Meng Wang	Zhihui Wang	Qi Yang	Qing Yue	Lijie Zhang
Ying Zhang	Lishu Zheng				

Editor in Charge Nankun Liu

Cover Image: credited from the Jufen Liu research team.
This week's issue was organized by Guest Editor Jufen Liu.

Vital Surveillances

Evaluation of Perinatal Prevalence, Geographic Disparities, and Survival of Neural Tube Defects — China, 2006–2024

Wenli Xu[1]; Wenyan Li[1]; Jufen Liu[2]; Yuyan Gao[1]; Zhiyu Chen[1]; Xuelian Yuan[1]; Qi Li[1]; Jun Zhu[1,3,4]; Xiaohong Li[4,5,#]; Li Dai[1,3,6,#]

ABSTRACT

Introduction: Neural tube defects (NTDs) are a major cause of perinatal mortality and lifelong disability. However, long-term trends in NTD prevalence, regional disparities, and survival patterns in China remain poorly characterized.

Methods: Data from the Chinese Birth Defects Monitoring Network (CBDMN) were analyzed for perinatal NTDs occurring between 2006 and 2024. Bayesian Poisson regression models incorporating subtype, geographic strata, maternal age, calendar year, and interaction effects were applied to estimate long-term trends in perinatal prevalence and survival. Joinpoint analysis was employed to estimate annual percentage changes (APCs).

Results: The estimated perinatal prevalence of NTDs in China declined from 8.84 per 10,000 births in 2006 to 0.77 per 10,000 births in 2024, representing a 91.29% reduction. Joinpoint analysis identified a three-phase decline pattern, with the APC accelerating from −10.43% (2006–2009) to −16.08% (2009–2016), followed by a slower decline of −10.60% (2016–2024). Similar downward trends were observed across all major NTD subtypes, with anencephaly showing the steepest decline. Long-standing nationwide north-south and urban-rural gaps in NTD prevalence were greatly reduced, with no statistically distinguishable differences observed during the late study period. Meanwhile, overall perinatal survival increased from 23.33% to 46.76%, driven primarily by marked improvements in spina bifida and encephalocele survival.

Conclusion: From 2006 to 2024, China demonstrated a remarkable decline in perinatal NTD prevalence, alongside a substantial narrowing of the long-standing national north-south and urban-rural gaps in disease burden. The increasing perinatal survival among nonlethal subtypes highlights the emerging need for long-term pediatric care and rehabilitation.

Neural tube defects (NTDs), one of the most prevalent birth defects, are a major cause of perinatal mortality and lifelong childhood disability worldwide (*1*). In the 1980s, NTDs had a high perinatal prevalence of 27 per 10,000 births, ranking first among all types of congenital malformations in China, with striking north-south and urban-rural disparities (*2*). The 1995 promulgation of the Law on Maternal and Infant Health Care of the People's Republic of China legalized national birth defect prevention and control. The Working Committee on Women and Children under the State Council issued the Outline for Chinese Children's Development (2001–2020), which for the first time included "reducing the incidence of birth defects" in government work targets (*3*). Since 2003, the rapid popularization of prenatal ultrasonography has allowed more NTD cases to be diagnosed prenatally (*4*). Following the national basic public health service equalization reform initiated in 2008, China implemented key preventive strategies, including free folic acid supplementation (2009) and free pre-pregnancy health screening for rural residents (2011) (*5*–*6*). These interventions have substantially reduced the occurrence of NTDs and reshaped their epidemiological profiles nationwide. Previous epidemiological studies have documented a substantial decrease in the perinatal prevalence of NTDs in China over the past decade (*7*). However, research on the temporal dynamics of north-south variations and urban-rural disparities in NTDs, along with the long-term trends in perinatal survival, remains limited. Herein, data from the Chinese Birth Defects Monitoring Network (CBDMN) was utilized to assess the temporal trends, geographic disparities, and perinatal survival rates of NTDs from 2006 to 2024, with the aim of providing robust epidemiological evidence for optimizing national NTD prevention and control strategies in China.

Copyright © 2026 by Chinese Center for Disease Control and Prevention

METHODS

Data were obtained from the CBDMN, a nationwide hospital-based surveillance system covering 786 hospitals across 326 counties or districts in 31 provincial-level administrative divisions (PLADs) in China. The CBDMN routinely collects data on the number of live births and stillbirths from all participating hospitals. All births delivered at monitoring hospitals with birth defects diagnosed during the perinatal period (28 gestational weeks to 7 days after birth) are mandatorily reported and coded according to the Tenth Revision of the International Classification of Diseases (ICD-10). The CBDMN annually monitors approximately 10% of all births in China. The annual numbers of monitored births are listed in Supplementary Table S1 (available at https://weekly.chinacdc.cn/). Data were collected using standardized national protocols with multilevel quality control at the hospital, provincial, and national levels (*8*–*9*).

NTD cases were classified into three major subtypes: anencephaly (ICD-10: Q00), encephalocele (Q01), and spina bifida (Q05). The urban-rural classification was based on maternal residence; northern and southern China were defined by the Qinling Mountain–Huaihe River Line (*10*). The original monitoring data were sorted and restructured to establish a dataset for analysis. The variables included in the final dataset were calendar year (variable name: t; 2006–2024), geographic and urban-rural stratification (x_1; north-urban, north-rural, south-urban, and south-rural), NTD subtype (x_2), maternal age group (x_3; <20, 20–24, 25–29, 30–34, and ≥35 years), number of births (n_lbs), number of affected cases (y_1), and number of affected cases surviving within 7 days after birth (y_2).

Perinatal prevalence was defined as the NTD case count per 10,000 perinatal births. Perinatal survival was defined as the 7-day postnatal survival proportion of NTD-affected cases. Bayesian Poisson regression models were applied to estimate the annual perinatal NTD prevalence and survival rates stratified by geography (north *vs.* south) and residence (urban *vs.* rural). For the prevalence estimation model, a log link function was applied for the dependent variable y_1 with an offset term $\exp(n_lbs)$. Predictors included time t and t^2; covariates x_1, x_2, and x_3; and interaction terms x_1t and x_2t. For the perinatal survival rate estimation model, as several subgroups contained no NTD exposures and thus had zero denominators for calculating survival rates, cases and survival events were pooled across age groups to ensure reliable model estimation. $\text{Log}(y_2)$ with y_1 as the offset and predictors t, t^2, x_1, x_2, x_1t, and x_2t were used. Interaction terms were incorporated, given the distinct temporal trends in NTD prevalence and perinatal survival across subtypes, regions, and urban-rural settings (*11*). Bayesian estimates of NTD prevalence and survival rates with 95% uncertainty intervals (*UI*s) were obtained from 10,000 Markov Chain Monte Carlo posterior samples. Joinpoint regression was applied to identify temporal changes and estimate phase-specific annual percentage changes (APCs).

Bayesian analyses were performed using Stata (version 17.0; StataCorp LLC, College Station, Texas, USA), and Joinpoint regression analyses were conducted using the Joinpoint Regression Program (version 6.0.1; National Cancer Institute, Bethesda, MD, USA).

RESULTS

The estimated perinatal prevalence of NTDs in China declined from 8.84 per 10,000 births in 2006 to 0.77 per 10,000 births in 2024, representing an overall reduction of 91.29% (Figure 1). Joinpoint analysis identified two statistically significant inflection points in 2009 and 2016, defining three consecutive trend segments (2006–2009, 2009–2016, and 2016–2024), with the APC accelerating from −10.43% during 2006–2009 to a peak of −16.08% during 2009–2016, followed by a slower decline of −10.60% during 2016–2024 (Table 1). Similar trends were observed for all major NTD subtypes. Anencephaly consistently demonstrated the steepest annual reduction across all periods. Spina bifida remained the predominant subtype, with its prevalence decreasing from 4.90 to 0.54 per 10,000 births during 2006–2024. The prevalence of anencephaly declined from 2.57 to 0.14 per 10,000 births, while that of encephalocele decreased from 1.39 to 0.09 per 10,000 births.

Marked reductions in north-south and urban-rural disparities in NTD prevalence were observed (Figure 2). In 2006, the prevalence in northern China was higher than that in southern China (12.56 *vs.* 5.43 per 10,000 births), with a corresponding prevalence ratio of 2.31 (95% *UI*: 1.92, 2.81). By 2024, the prevalence decreased to 0.73 per 10,000 births in the north and 0.80 per 10,000 births in the south, with a prevalence ratio of 0.90 (95% *UI*: 0.62, 1.28). Similarly, the estimated prevalence in rural areas

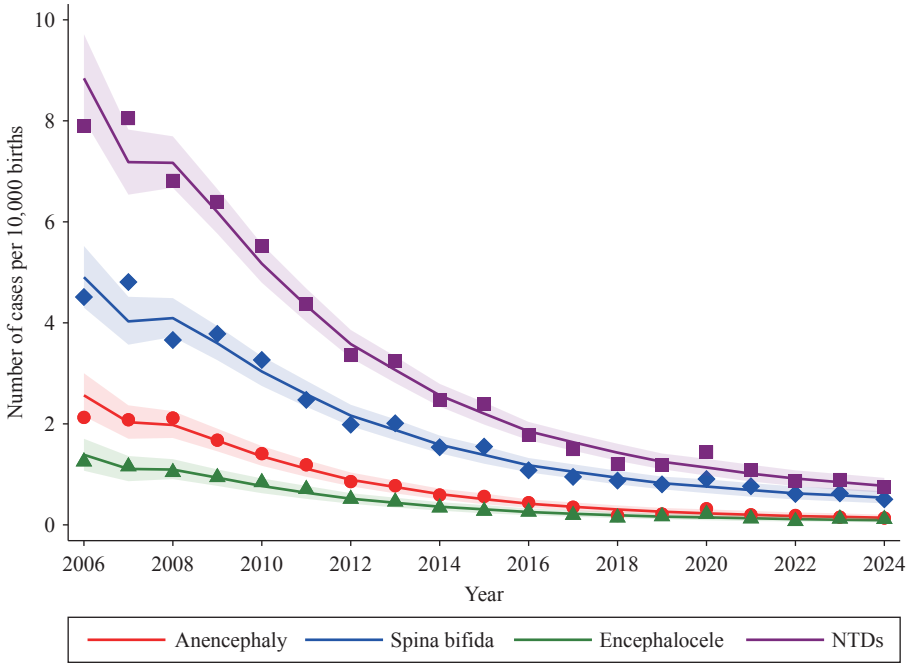

FIGURE 1. Temporal trends in perinatal prevalence of neural tube defects and major subtypes in China, 2006–2024.
Note: Dots represent observed rates, and solid lines represent Bayesian posterior median estimates.
Abbreviation: NTDs=Neural tube defects.

TABLE 1. Annual percentage change in the perinatal prevalence of all neural tube defects and the major subtypes across three study periods in China, 2006–2024.

Phenotype	Stage 1 (2006–2009)	Stage 2 (2009–2016)	Stage 3 (2016–2024)
Anencephaly	−12.60 (−14.85, −8.78)	−18.17 (−20.65, −17.35)	−13.01 (−14.60, −10.20)
Spina bifida	−9.04 (−11.48, −4.86)	−14.95 (−17.19, −14.14)	−9.55 (−10.89, −7.56)
Encephalocele	−11.59 (−13.95, −7.44)	−17.19 (−19.82, −16.35)	−12.05 (−13.61, −9.35)
Total NTDs	−10.43 (−12.79, −6.54)	−16.08 (−18.35, −15.27)	−10.60 (−12.01, −8.53)

Note: Values in parentheses represent the 95% confidence intervals.
Abbreviation: NTDs=Neural tube defects.

(16.27 per 10,000 births) was nearly three times higher than that in urban areas (4.99 per 10,000 births) in 2006. By 2024, the urban-rural prevalence ratio had declined to 1.29 (95% *UI*: 0.89, 1.84), with the 95% *UI* including 1, suggesting no statistically significant urban-rural gap in NTD prevalence.

The estimated NTD perinatal survival rate substantially increased during the study period (Figure 3). By subtype, the perinatal survival rate of anencephaly remained persistently low (<10.00%). In comparison, the survival rate improved markedly for spina bifida (30.43% to 54.84%) and encephalocele (27.71% to 57.14%). The overall NTD perinatal survival rate increased from 23.33% to 46.76% during the study period. Perinatal survival rate improvements were observed in both urban (from 25.46% to 49.40%) and rural (21.82% to 41.07%) settings, with rates being slightly higher in urban *vs.* rural populations. Given the substantial overlap of the 95% *UIs*, no statistically significant urban-rural differences were observed (Supplementary Figure S1, available athttps://weekly.chinacdc.cn/).

DISCUSSION

This study extends previous national surveillance studies by applying Bayesian methods to characterize the long-term trends in NTD prevalence, geographic disparities, and perinatal survival (*9*,*12*). The results revealed substantial reductions in NTD prevalence and geographic disparities, along with improvements in perinatal survival over time. These findings reflect a shift in public health priorities, transitioning from primary incidence reduction to enhanced clinical management and supportive care for NTD survivors.

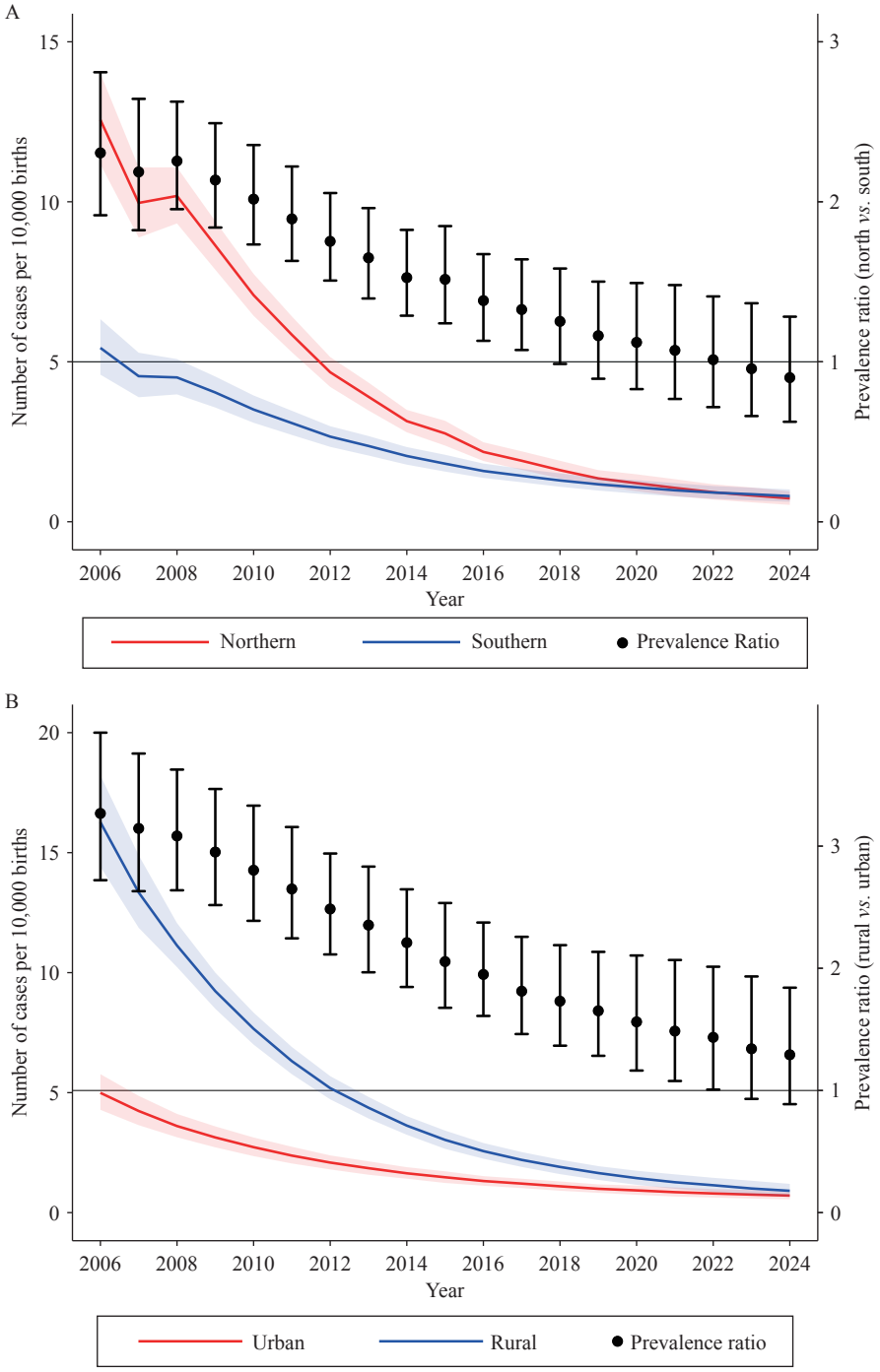

FIGURE 2. Geographic and urban-rural differences in the perinatal neural tube defect prevalence in China, 2006–2024. (A) North-south differences. (B) Urban-rural differences.
Abbreviation: NTD=Neural tube defect.

China's rapid decline in perinatal NTD prevalence may have been driven by the nationwide expansion and improvement of birth defect prevention and control measures. Since 2009, nationwide folic acid supplementation programs have progressively expanded from rural to urban areas. From 2000–2004 to 2011–2012, periconceptional folic acid use increased from 15% to 85% in high-NTD-prevalence areas and from 66% to 92% in low-prevalence areas (*13*). The free pre-pregnancy health screening program was piloted in 100 counties in 2010. It had expanded to all counties and districts across China by 2013, covering rural couples planning pregnancy with a target population coverage rate of >80%. By 2016, the

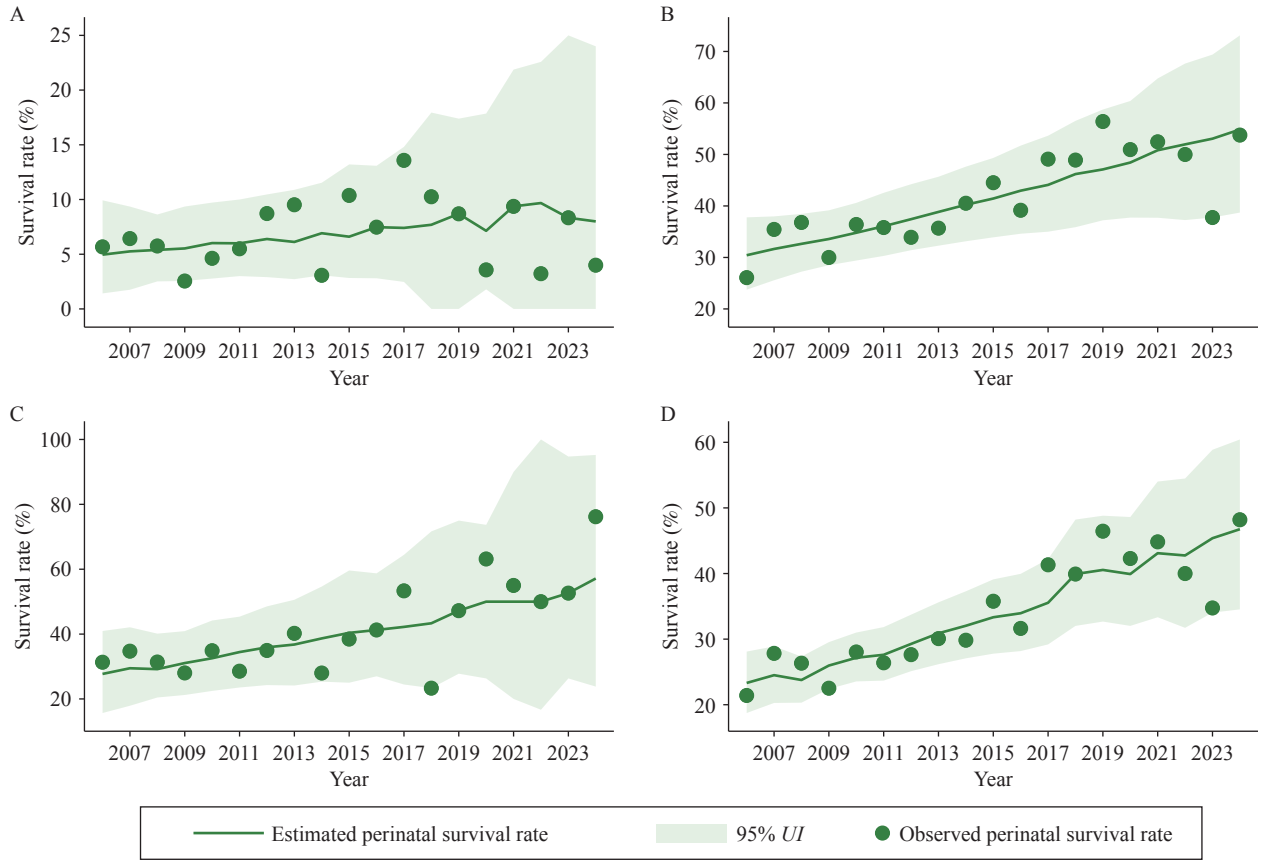

FIGURE 3. Temporal trends in perinatal survival rates of all neural tube defects and the major subtypes in China, 2006–2024. The panels show the survival rates for (A) anencephaly, (B) spina bifida, (C) encephalocele, and (D) NTDs.
Note: Dots represent observed rates, and solid lines represent Bayesian posterior median estimates.
Abbreviation: NTDs=Neural tube defects; *UI*=Uncertainty interval.

coverage rate had increased to 93.5%. The quick growth in coverage may explain the rapid decline in NTD prevalence (*7*). The first National Health Industry Standard for prenatal NTD screening and diagnosis was released in 2010. The 2012 guidelines promoting universal prenatal ultrasound screening, especially for severe anomalies, significantly improved the ability of prenatal screening institutions to detect NTDs. By 2020, second-trimester ultrasound screening coverage exceeded 80%, and maternal serum alpha-fetoprotein screening coverage for NTDs increased from 8.4% (2007) to 65.9% (2020) (*14*). These interventions were initially implemented between 2009 and 2012, likely explaining the rapid decline in NTD prevalence that was observed during this period.

Globally, the NTD prevalence has declined substantially, particularly in countries implementing folic acid fortification and maternal health interventions. For example, following mandatory folic acid fortification, the United States and Canada reported marked declines in NTD prevalence, with recent estimates stabilizing at approximately 4–7 per 10,000 births. Beyond these interventions, growing evidence indicates that comprehensive pre-conception care may further reduce the risk of structural birth defects (*15*–*16*). However, international comparisons should be interpreted cautiously, because surveillance definitions differ substantially. Most countries report the total birth prevalence across all gestational ages, potentially leading to lower observed prevalence estimates.

Historical NTD disparities in northern and rural China likely reflected underlying biological, health awareness, environmental, nutritional, and healthcare factors, as they predated widespread prenatal screening (*10*). With socioeconomic progress and ongoing efforts to equalize public health services nationwide, the universal use of folic acid, better nutrition, and improved maternal and child healthcare services have jointly reduced the north-south and urban-rural disparities attributed to uneven dietary conditions and

healthcare accessibility (*3*,*5*). Moreover, cross-regional population mobility and population intermixing may have modestly diluted historically localized genetic susceptibilities, although this hypothesis warrants further investigation (*17*). However, improved prenatal diagnosis and early termination may have contributed to the observed North-South and urban-rural differences in perinatal NTD prevalence in the last decade. Nevertheless, it remains unclear whether these NTD prevalence gaps have been completely eliminated at the economic or provincial level.

The increased survival among non-lethal NTD subtypes reflects a shift in public health priorities from mortality prevention to long-term care. These improvements likely resulted from advances in fetal anomaly screening, prenatal diagnosis, perinatal management, and neonatal surgery (*18*). As NTD cases become increasingly rare, annual survival estimates become more susceptible to random variations and should be interpreted cautiously.

This study has some limitations. First, potential selection bias may exist owing to the hospital-based surveillance design. Second, the effects of specific prevention policies could not be evaluated quantitatively. Third, the north-south classification may not capture provincial-level heterogeneity.

In conclusion, from 2006 to 2024, China demonstrated substantial reductions in the prevalence of perinatal NTD, with marked reductions in geographic and socioeconomic disparities. Future public health programs may need to focus on addressing residual risk factors while expanding long-term rehabilitation and supportive care.

Conflicts of interest: No conflicts of interest.

Acknowledgments: All colleagues from local institutions for participating in data collection.

Ethical statement: The data used in this study were obtained from the national surveillance system for birth defects. This study was approved by the Ethics Committee of West China Second University Hospital (No. 2026(143)).

Funding: Supported by the National Key Research and Development Program of China (Grant No. 2025YFC2511501).

doi: 10.46234/ccdcw2026.189

[#] Corresponding authors: Xiaohong Li, lixiaohong82@scu.edu.cn; Li Dai, daili@scu.edu.cn.

[1] National Center for Birth Defects Monitoring, West China Second University Hospital, Sichuan University, Chengdu City, Sichuan Province, China; [2] Institute of Reproductive and Child Health/National Health Commission Key Laboratory of Reproductive Health, Department of Epidemiology and Biostatistics, School of Public Health, Peking University, Beijing, China; [3] Key Laboratory of Birth Defects and Related Diseases of Women and Children (Sichuan University), Ministry of Education, Chengdu City, Sichuan Province, China; [4] Sichuan Birth Defects Clinical Research Center, West China Second University Hospital, Sichuan University, Chengdu City, Sichuan Province, China; [5] Children's Medicine Key Laboratory of Sichuan Province, West China Second University Hospital, Sichuan University, Chengdu City, Sichuan Province, China; [6] Medical Big Data Center, Sichuan University, Chengdu City, Sichuan Province, China.

Copyright © 2026 by Chinese Center for Disease Control and Prevention & Chinese Academy of Preventive Medicine. All content is distributed under a Creative Commons Attribution Non Commercial License 4.0 (CC BY-NC).

Submitted: June 18, 2026
Accepted: August 16, 2026
Issued: September 18, 2026

REFERENCES

1. Bai ZH, Han JR, An J, Wang H, Du XY, Yang ZC, et al. The global, regional, and national patterns of change in the burden of congenital birth defects, 1990-2021: an analysis of the global burden of disease study 2021 and forecast to 2040. eClinicalMedicine 2024;77:102873. https://doi.org/10.1016/j.eclinm.2024.102873.
2. Xiao KZ, Zhang ZY, Gao J, Liu FQ, Rao HL, Jiang ZQ, et al. Epidemiology of neural tube defects in China. Natl Med J China 1989;69(4):189-91. http://dx.doi.org/10.3760/cma.j.issn.0376-2491.1989.04.103. (In Chinese).
3. Qiao J, Wang YY, Li XH, Jiang F, Zhang YT, Ma J, et al. A *Lancet* Commission on 70 years of women's reproductive, maternal, newborn, child, and adolescent health in China. Lancet 2021;397(10293):2497 – 536. https://doi.org/10.1016/S0140-6736(20)32708-2.
4. Wang LL, Du J. Advances in prenatal diagnosis and intrauterine treatment of neural tube defects. Chin J Prenat Diag (Electron Vers) 2013;5(1):23-7. http://dx.chinadoi.cn/10.3969/j.issn.1674-7399.2013.01.007. (In Chinese).
5. Wang QM. Maternal and child health promotion and birth defects prevention and treatment strategies. Chin J Woman Child Health Res 2020;31(9):1129 – 31. https://doi.org/10.3969/j.issn.1673-5293.2020.09.001.
6. Song L. Maternal and child health in Healthy China: progress and prospects of maternal and child health promotion actions. Healthy China Obs 2023;(8):34-7. http://lib.cqvip.com/Qikan/Article/Detail?id=7110385250&from=Qikan_Search_Index. (In Chinese).
7. Kancherla V. Neural tube defects: a review of global prevalence, causes, and primary prevention. Child's Nerv Syst 2023;39(7):1703 – 10. https://doi.org/10.1007/s00381-023-05910-7.
8. Dai L, Zhu J, Liang J, Wang YP, Wang H, Mao M. Birth defects surveillance in China. World J Pediatr 2011;7(4):302 – 10. https://doi.org/10.1007/s12519-011-0326-0.
9. Xu WL, Deng CF, Li WY, Wang K, Tao J, Gao YY, et al. National perinatal prevalence of selected major birth defects — China, 2010–2018. China CDC Wkly 2020;2(37):711 – 7. https://doi.org/10.46234/ccdcw2020.195.
10. Li XH, Zhu J, Wang YP, Mu DZ, Dai L, Zhou GX, et al. Geographic and urban-rural disparities in the total prevalence of neural tube defects and their subtypes during 2006-2008 in China: a study using the hospital-based birth defects surveillance system. BMC Public Health 2013;13(1):161. https://doi.org/10.1186/1471-2458-13-161.
11. Achcar JA, Martinez EZ, de Souza ADP, Tachibana VM, Flores EF. Use of Poisson spatiotemporal regression models for the Brazilian Amazon Forest: malaria count data. Rev Soc Bras Med Trop 2011;44(6):749 – 54. https://doi.org/10.1590/S0037-86822011000600019.

12. Li WY, Chen ZY, Xu WL, Gao YY, Liu Z, Li Q, et al. Temporal trends in the prevalence of major birth defects in China: a nationwide population-based study from 2007 to 2021. World J Pediatr 2024;20 (11):1145 – 54. https://doi.org/10.1007/s12519-024-00844-9.
13. Liu JF, Jin L, Meng QQ, Gao LL, Zhang L, Li ZW, et al. Changes in folic acid supplementation behaviour among women of reproductive age after the implementation of a massive supplementation programme in China. Public Health Nutr 2015;18(4):582 – 8. https://doi.org/10.1017/S1368980014000950.
14. Department of Maternal and Child Health NHCoC. National fourth survey on prenatal screening and prenatal diagnosis services in China. Beijing: National Health Commission. 2021. https://www.mchscn.cn/Textnews-13/632.html. (In Chinese).
15. Doe PF, Nimo FA, Odoom E, Asore MA, Alhassan A, Lanyo GS, et al. Couple-based preconception care as a gender-responsive strategy for improving health and well-being: a systematic review. Reprod Health 2026;23(1):159. https://doi.org/10.1186/s12978-026-02385-y.
16. Shannon GD, Alberg C, Nacul L, Pashayan N. Preconception healthcare and congenital disorders: systematic review of the effectiveness of preconception care programs in the prevention of congenital disorders. Matern Child Health J 2014;18(6):1354 – 79. https://doi.org/10.1007/s10995-013-1370-2.
17. Niu XY, Liu SH, Zhu Y. Spatial characteristics of China's urbanization: the perspective of inter-prefecture population movement. Urban Plann Forum 2021(1):82 – 9. https://doi.org/10.16361/j.upf.202100010.
18. Birth Defects Prevention and Molecular Genetics Branch of the China Maternal and Child Health Association, Pediatric Genetics Group of the Medical Genetics Physicians Branch of the Chinese Medical Doctor Association, Neurogenetic and Developmental Disorders Section of the China Chapter of the International Neurorestoration Society. Multidisciplinary expert consensus on the prevention, screening, diagnosis, counseling and intervention of neural tube defects. J Clin Pediatr 2025;43(2):81 – 92. https://doi.org/10.12372/jcp.2025.24e0672.

SUPPLEMENTARY MATERIALS

SUPPLEMENTARY TABLE S1. Annual number of births and NTD cases by geographic region in China, 2006–2024.

Year	Total births	North China births	South China births	Total NTD cases
2006	662,761	316,835	345,926	523
2007	821,468	397,376	424,092	661
2008	1,314,091	615,749	698,342	896
2009	1,401,331	658,900	742,431	897
2010	1,531,143	710,112	821,031	845
2011	1,681,096	766,755	914,341	735
2012	2,005,526	915,846	1,089,680	673
2013	1,893,854	859,802	1,034,052	615
2014	2,198,818	1,026,846	1,171,972	543
2015	1,883,843	760,598	1,123,245	450
2016	2,432,979	1,090,669	1,342,310	433
2017	2,315,621	986,088	1,329,533	346
2018	2,097,800	881,155	1,216,645	253
2019	2,143,629	922,797	1,220,832	254
2020	1,751,281	721,170	1,030,111	253
2021	1,596,171	661,292	934,879	174
2022	1,666,779	692,032	974,747	145
2023	1,572,552	643,425	929,127	141
2024	1,837,817	779,115	1,058,702	139

Abbreviation: NTD=Neural tube defect.

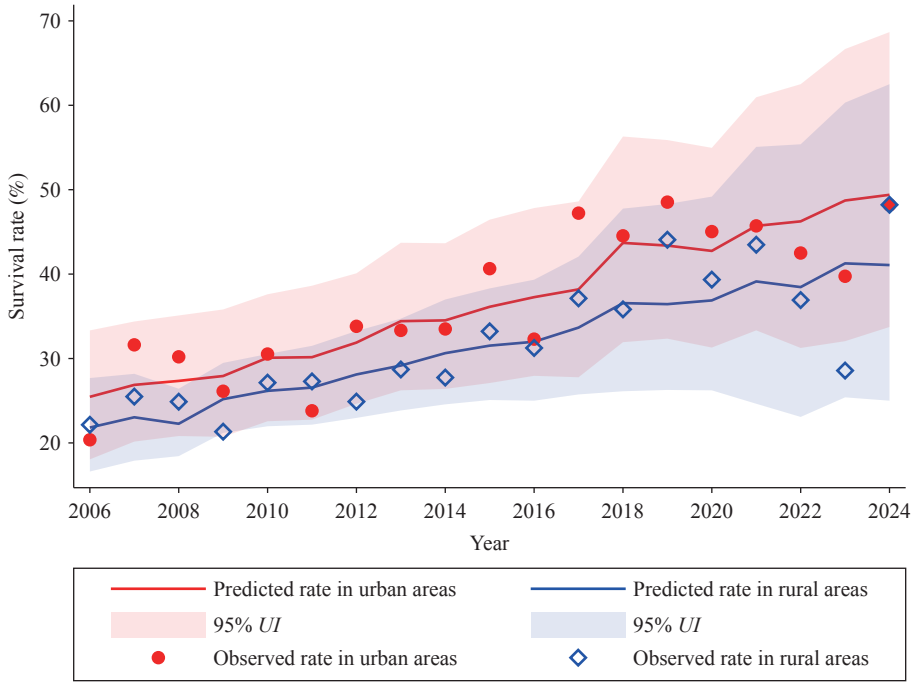

SUPPLEMENTARY FIGURE S1. Urban-rural differences in perinatal survival rates of all neural tube defects in China, 2006–2024.
Abbreviation: NTDs=Neural tube defects; *UI*=Uncertainty interval.

Preplanned Studies

Shifting Burden of Neural Tube Defects from Early-Life Mortality to an Aging Population Living with Disability — China, 1990–2023

Yuwei Wu[1,2]; Xiaoqian Jia[1,2]; Lingzhang Wang[1,2]; Xinyue Lin[1,2]; Yali Zhang[1,2]; Le Zhang[1,2]; Zhiwen Li[1,2,3]; Zhiyong Zou[4,#]; Jufen Liu[1,2,3,#]

Summary

What is already known about this topic?

The burden of neural tube defects (NTDs) has declined with folic acid supplementation and fortification, but comprehensive all-age estimates are lacking.

What is added by this report?

Using data from the Global Burden of Disease Study 2023, we assessed the all-age NTD burden in China during 1990–2023. Incidence, mortality, and disability-adjusted life year (DALY) rates declined significantly, whereas prevalence increased among adults aged ≥50 years and DALY rates increased among those aged ≥75 years, indicating a shift from early-life mortality to disability in an aging population.

What are the implications for public health practice?

Life-course care should combine primary prevention, long-term rehabilitation and multidisciplinary management for people with NTDs.

ABSTRACT

Background: Although the perinatal burden of neural tube defects (NTDs) has declined, comprehensive all-age burden assessments in China and sociodemographic index (SDI) quintiles are lacking.

Methods: Using data from the Global Burden of Diseases, Injuries, and Risk Factors Study 2023, we analyzed NTD burden trends in China and five SDI quintiles during 1990–2023. Rate trends were assessed using estimated annual percentage changes (EAPCs) and Joinpoint-derived average annual percentage changes (AAPCs).

Results: In China, NTD incidence, mortality, and disability-adjusted life year (DALY) rates decreased significantly during 1990–2023, whereas the prevalence rate showed no significant change. Within China, all three rates declined more among men than among women, and incidence and mortality rates declined most sharply among children aged <5 years. Age-specific EAPC analyses in China showed increasing prevalence and DALY rates among adults aged ≥50 years. In 2023, China's SDI was within the high-SDI range; over 1990–2023, reductions in its incidence, mortality, and DALY rates exceeded those in every SDI quintile. Joinpoint-derived AAPCs further showed increasing DALY rates among adults aged ≥75 years in China and the high-middle-SDI quintile and among those aged ≥50 years in the high-SDI quintile.

Conclusion: The NTD burden in China has declined since 1990, but a shift toward older age groups highlights the need for integrated life-course care and sustained prevention.

Neural tube defects (NTDs) are serious congenital anomalies associated with perinatal mortality and lifelong disability. Globally, birth defects burden has decreased, particularly in regions with a low sociodemographic index (SDI) (*1*). In China, folic acid supplementation has contributed to a decline in NTD birth prevalence from 5.3 to 0.5 per 10,000 between 2007 and 2021 (*2*). Meanwhile, rising years lived with disability suggest a shift toward nonfatal outcomes (*3*). Although, most studies have focused on perinatal burden of NTDs, improve survival, particularly among people with spina bifida, has resulted in aging population living with disability. A nationwide insurance claims–based study estimated that at least 92,551 people in the United States were living with spina bifida in 2019, with prevalence documented across all adult age groups, including those aged ≥65 years (*4*). Comprehensive all-age assessments in China and comparisons across SDI quintiles remain lacking.

Copyright © 2026 by Chinese Center for Disease Control and Prevention

Using the Global Burden of Diseases, Injuries, and Risk Factors Study 2023 (GBD 2023), we analyzed all-age NTD burden by sex and age in China during 1990–2023, with five SDI quintiles as contextual comparators.

Absolute numbers and rates of incidence, prevalence, mortality, and disability-adjusted life years (DALYs) for NTDs in China and across the five SDI quintiles were extracted from the GBD 2023 (*5*). Data are publicly available through the Global Health Data Exchange (GHDx) GBD Results Tool https://vizhub.healthdata.org/gbd-results/. The SDI is a composite index ranging from 0 to 1 and based on fertility among those younger than 25 years, education among those aged 15 years and older, and lag-distributed income per capita (*5*). Based on 2023 values, locations were categorized as low-SDI (0.0000–0.5316), low-middle-SDI (0.5316–0.6305), middle-SDI (0.6305–0.6767), high-middle-SDI (0.6767–0.7188), and high-SDI (0.7188–1.0000) (https://ghdx.healthdata.org/record/gbd-2023-socio-demographic-index-sdi). Examples are provided in Supplementary Table S1 (available at https://weekly.chinacdc.cn). Although GBD 2023 does not explicitly assign China to a category, its 2023 SDI was estimated at 0.7275, within the high-SDI range. DALYs were calculated as years of life lost plus years lived with a disability. Rates were age-standardized to the GBD world standard population (*5*). Burden trends from 1990 to 2023 were analyzed by sex and age in China and compared the five SDI quintiles.

Statistical significance was defined as a two-sided α level of 0.05. Percentage changes in absolute numbers from 1990 to 2023 and 95% uncertainty intervals (*UI*s) were estimated using the delta method. Rate trends were assessed using estimated annual percentage changes (EAPCs) with 95% *UI*s from log-linear models. Joinpoint regression (version 5.4.0; National Cancer Institute, Bethesda, MD, USA) identified changes in trend slope, allowing a maximum of 4 joinpoints and using permutation tests (α=0.05). Segment-specific annual percentage changes (APCs) and average annual percentage changes (AAPCs) for 1990–2023 were calculated. Additional analyses and graphics were generated using R, version 4.5.2 (R Foundation for Statistical Computing, Vienna, Austria). Detailed ICD definitions, formulas, and age-standardization methods are provided in the Supplementary Materials.

In China, the numbers of incident cases, prevalent cases, deaths, and DALYs in 2023 were 3,258.36 (95% *UI*: 2,842.75–3,694.51), 71,879.03 (95% *UI*: 59,349.41–86,825.24), 411.22 (95% *UI*: 284.88–570.67), and 55,780.00 (95% *UI*: 41,672.03–71,605.38), respectively (Table 1). Compared with 1990, these numbers decreased by 88.75% (95% *UI*: 88.72–88.78), 33.95% (95% *UI*: 33.73–34.16), 97.31% (95% *UI*: 97.29–97.32), and 96.00% (95% *UI*: 95.98–96.03), respectively. Incidence, mortality, and DALY rates declined significantly, with EAPCs of −4.17 (95% *UI:* −4.81 to −3.52), −10.61 (95% *UI:* −11.48 to −9.73), and −9.96 (95% *UI*: −10.76 to −9.15), respectively; prevalence showed no significant change (EAPC: 0.11, 95% *UI:* −0.49 to 0.72). Age-standardized incidence, mortality, and DALY rates were higher in men in 1990 but higher in women by 2023, reflecting steeper declines in men (Supplementary Table S2, available at https://weekly.chinacdc.cn). Age-specific EAPCs were heterogeneous (Supplementary Table S3, available at https://weekly.chinacdc.cn). Incidence and mortality rates declined most sharply among children aged <5 years. Prevalence rate showed no significant trend among persons aged ≤ 49 years but increased among those aged ≥50 years. Mortality rate declined in all age groups aged ≤ 74 years, while DALY rates declined among those aged ≤ 49 years but increased among those aged ≥50 years.

Table 1 presents NTD burden across the five SDI regions and China. Temporal trends are shown in Figure 1A–D. In both 1990 and 2023, the age-standardized incidence rates were highest in the low-SDI regions and lowest in the high-SDI regions. All SDI quintiles recorded significant declines, greatest in the high-middle-SDI regions (EAPC: −3.10, 95% *UI:* −3.34 to −2.85) and the smallest in the low-SDI regions (EAPC: −1.37, 95% *UI:* −1.45 to −1.29), while China experienced a greater decline (EAPC: −4.17, 95% *UI:* −4.81 to −3.52). Regarding prevalence, the steepest decline was observed in low-middle-SDI regions (EAPC: −1.23, 95% *UI:* −1.32 to −1.13), whereas high-SDI regions showed a non-significant increase. China's EAPC for prevalence was not statistically significant; rates decreased during 1990–1999, rose after 2005, and remained below all SDI quintiles throughout the study period. Age-standardized mortality rates fell across all SDI quintiles, were inversely associated with SDI, and declined more steeply at higher SDI regions (EAPC: −5.15, 95% *UI:* −5.44 to −4.85 in high-SDI *vs.* −1.52,

TABLE 1. Burden of NTDs for China and five SDI quintiles, 1990–2023.

Indicator	Group	Absolute number† (95% *UI*)			Age-standardized rates/100,000 (95% *UI*)		
		1990	2023	Percentage change (%)	1990	2023	EAPC
Incidence	China	28,967.67 (23124.54, −34854.15)	3,258.36 (2842.75, 3694.51)	−88.75 (−88.78, −88.72)	2.66 (2.12, 3.20)	0.73 (0.64, 0.83)	−4.17 (−4.81, −3.52)*
	Low-SDI	76,560.79 (63,623.45, 90,374.77)	79,182.30 (68,659.65, 90,100.85)	3.42 (3.20, 3.65)	4.84 (4.02, 5.71)	3.29 (2.85, 3.74)	−1.37 (−1.45, −1.29)*
	Low-middle-SDI	36,009.72 (29,721.27, 42,536.86)	17,930.44 (15,417.32, 20,478.35)	−50.21 (−50.32, −50.09)	3.33 (2.75, 3.93)	1.72 (1.48, 1.96)	−2.27 (−2.38, −2.15)*
	Middle-SDI	19,629.15 (16,230.39, 23,289.35)	8,120.66 (6,986.24, 9,291.53)	−58.63 (−58.72, −58.53)	2.40 (1.99, 2.85)	1.05 (0.91, 1.21)	−2.73 (−2.85, −2.62)*
	High-middle-SDI	31,131.38 (25,663.69, 36,583.50)	7,831.33 (6,805.87, 8,858.02)	−74.84 (−74.90, −74.79)	2.50 (2.06, 2.94)	0.94 (0.82, 1.07)	−3.10 (−3.34, −2.85)*
	High-SDI	25,490.93 (21,273.72, 29,478.13)	8,285.07 (7,274.61, 9,173.46)	−67.50 (−67.56, −67.43)	1.60 (1.34, 1.85)	0.80 (0.70, 0.88)	−2.08 (−2.46, −1.71)*
Prevalence	China	108,818.21 (83,544.31, 139,848.11)	71,879.03 (59,349.41, 86,825.24)	−33.95 (−34.16, −33.73)	9.01 (6.91, 11.56)	6.65 (5.49, 7.98)	0.11 (−0.49, 0.72)
	Low-SDI	287,742.19 (240,018.50, 340,822.68)	468,114.72 (394,972.98, 546,796.62)	62.69 (62.30, 63.07)	27.02 (22.57, 31.91)	22.37 (18.92, 26.03)	−0.73 (−0.79, −0.66)*
	Low-middle-SDI	187,472.55 (155,545.61, 221,424.44)	184,920.54 (154,325.66, 21,313.60)	−1.36 (−1.60, −1.12)	21.50 (17.96, 25.49)	15.20 (12.72, 17.86)	−1.23 (−1.32, −1.13)*
	Middle-SDI	113,126.16 (92,390.47, 134,857.69)	107,154.03 (90,001.47, 126,420.37)	−5.28 (−5.52, −5.04)	15.64 (12.84, 18.67)	11.46 (9.60, 13.53)	−1.10 (−1.17, −1.04)*
	High-middle-SDI	185,446.24 (152,453.83, 225,297.93)	154,583.15 (130,357.10, 181,559.55)	−16.64 (−16.86, −16.43)	14.63 (12.04, 17.66)	10.74 (9.07, 12.60)	−0.87 (−0.95, −0.79)*
	High-SDI	238,132.61 (198,630.37, 284,527.19)	245,168.86 (208,170.91, 285,261.55)	2.95 (2.71, 3.20)	12.20 (10.15, 14.57)	11.62 (9.87, 13.56)	0.08 (−0.11, 0.27)
Mortality	China	15,262.52 (8,072.40, 24,418.03)	411.22 (284.88, 570.67)	−97.31 (−97.32, −97.29)	1.40 (0.74, 2.24)	0.08 (0.05, 0.11)	−10.61 (−11.48, −9.73)*
	Low-SDI	24,679.78 (12,022.23, 42,000.93)	24,914.49 (13,214.08, 43,143.28)	0.95 (0.09, 1.81)	1.64 (0.80, 2.78)	1.05 (0.56, 1.82)	−1.52 (−1.60, −1.43)*
	Low-middle-SDI	12,872.32 (6,503.18, 22,964.32)	6,610.61 (3,603.36, 12,818.25)	−48.64 (−49.13, −48.16)	1.22 (0.62, 2.19)	0.62 (0.34, 1.21)	−2.10 (−2.16, −2.05)*
	Middle-SDI	9,350.87 (5,600.80, 14,656.97)	4,875.24 (2,820.84, 8,000.74)	−47.86 (−48.24, −47.49)	1.16 (0.69, 1.81)	0.62 (0.36, 1.01)	−2.34 (−2.49, −2.19)*
	High-middle-SDI	15,496.72 (10,683.06, 21,740.86)	2,854.75 (1,945.55, 4,524.17)	−81.58 (−81.68, −81.47)	1.25 (0.86, 1.75)	0.32 (0.21, 0.50)	−4.95 (−5.22, −4.68)*
	High-SDI	13,118.72 (9,392.01, 17,175.00)	2,379.40 (2,058.16, 2,738.40)	−81.86 (−81.92, −81.80)	0.81 (0.58, 1.06)	0.20 (0.17, 0.23)	−5.15 (−5.44, −4.85)*
DALYs	China	1,395,231.49 (764,333.07, 2,213,112.98)	55,780.00 (41,672.03, 71,605.38)	−96.00 (−96.03, −95.98)	127.44 (69.40, 202.51)	8.58 (6.20, 11.57)	−9.96 (−10.76, −9.15)*
	Low-SDI	2,283,209.20 (1,158,363.55, 3,824,453.02)	2,353,059.59 (1,300,231.83, 3,979,568.38)	3.06 (2.22, 3.90)	152.82 (78.93, 253.73)	99.58 (55.23, 168.01)	−1.47 (−1.55, −1.39)*
	Low-middle-SDI	1,198,672.25 (632,670.89, 2,094,077.88)	639,258.65 (373,652.71, 1,193,086.20)	−46.67 (−47.14, −46.20)	114.52 (60.79, 199.70)	59.61 (34.53, 111.97)	−2.04 (−2.10, −1.99)*
	Middle-SDI	865,018.51 (538,477.93, 1,338,569.17)	462,595.77 (276,853.24, 741,231.94)	−46.52 (−46.89, −46.16)	107.18 (66.90, 165.42)	58.23 (34.67, 93.56)	−2.29 (−2.44, −2.15)*
	High-middle-SDI	1,431,006.70 (995,628.60, 1,980,713.32)	291,729.17 (212,474.68, 435,501.80)	−79.61 (−79.72, −79.51)	114.96 (79.96, 159.24)	30.89 (21.90, 47.53)	−4.73 (−4.99, −4.47)*
	High-SDI	1,226,489.11 (891,184.32, 1,597,333.63)	266,727.75 (228,514.79, 307,842.61)	−78.25 (−78.32, −78.18)	75.25 (54.43, 98.18)	20.47 (17.70, 23.53)	−4.76 (−5.05, −4.48)*

Abbreviation: NTDs=neural tube defect; SDI=sociodemographic index; EAPC=estimated annual percentage change; *UI*=uncertainty interval; DALYs=disability-adjusted life year.
* $P<0.05$.
† Absolute numbers represent incident cases, prevalent cases, deaths, and total DALYs, whereas rates represent incidence, prevalence, mortality, and DALY rates.

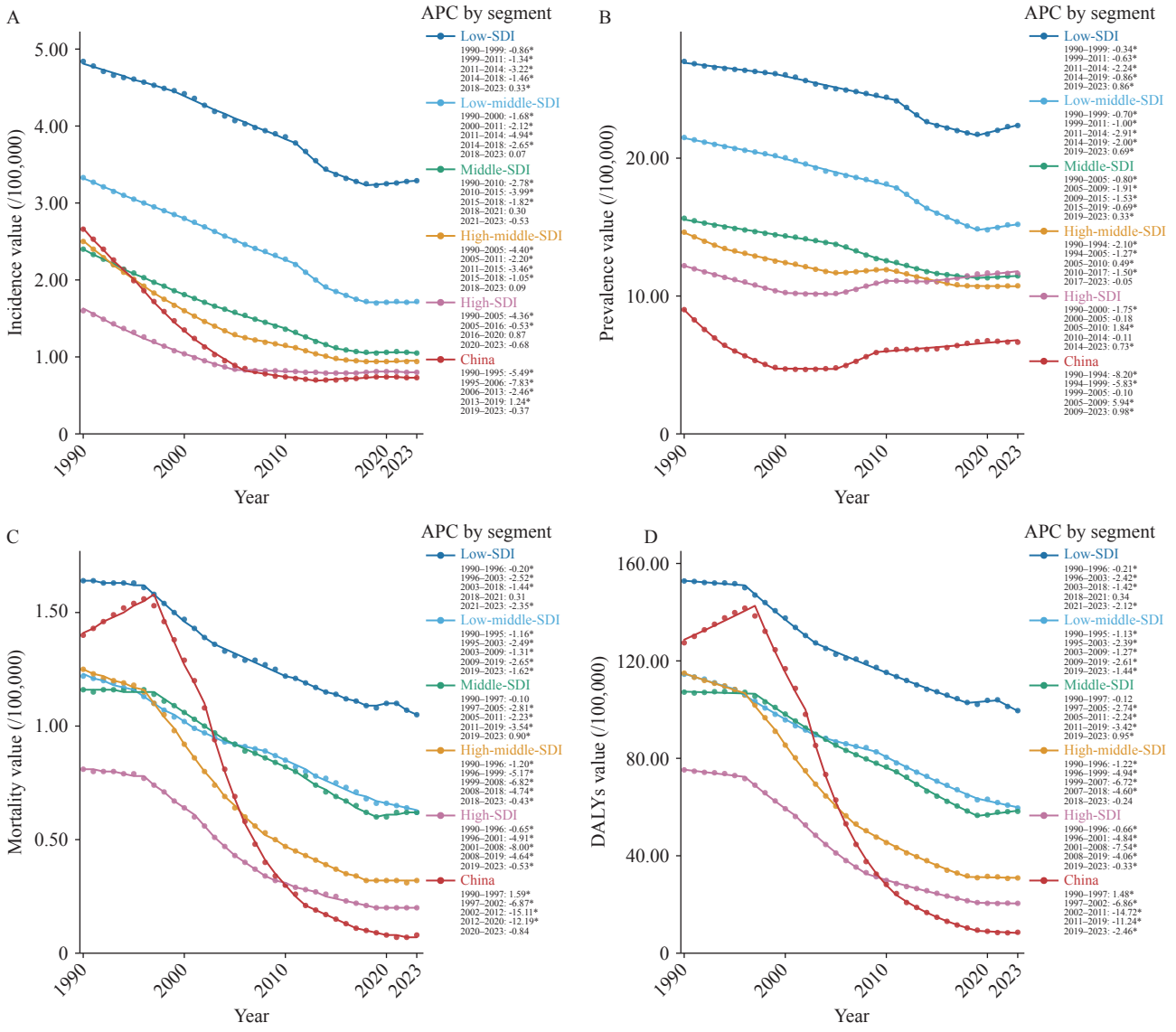

FIGURE 1. Age-standardized incidence, prevalence, mortality, DALY rates of NTDs for China and five SDI quintiles, 1990–2023. (A) Incidence; (B) Prevalence; (C) Mortality; and (D) DALYs.
Abbreviation: DALY=disability-adjusted life year; NTDs=neural tube defect; SDI=sociodemographic index; APC=annual percentage change.
* $P<0.05$.

95% *UI:* −1.60 to −1.43 in low-SDI). DALY rates were also inversely related to SDI, with greater declines at higher SDI regions (EAPC: −4.76, 95% *UI:* −5.05 to −4.48 in high-SDI *vs.* −1.47, 95% *UI:* −1.55 to −1.39 in low-SDI). China's DALY EAPC was −9.96 (95% *UI:* −10.76 to −9.15), a steeper reduction than across all SDI quintiles.

In China, the incidence and mortality rates have decreased in all age groups (Figure 2). The prevalence rate showed a downward trend among those under 50 years of age, while it showed an upward trend among those 50 years of age and older (AAPC: 1.40, 95% *UI*: 1.36–1.45 in 50–74 years age group; and 1.87, 95% *UI:* 1.82–1.92 in 75 years and above age group). The DALY rate showed a downward trend among individuals under 75 years of age, while it showed an upward trend among those 75 years of age and older (AAPC: 2.14, 95% *UI:* 2.09–2.19), consistent with the results of the EAPC fitting model. Analyses stratified by SDI quintile and age group further revealed that the prevalence of NTDs increased among individuals aged 50 years and older in the high-middle and high-SDI regions. The DALY rate for NTDs showed an upward trend among people aged 50 years and older in high-

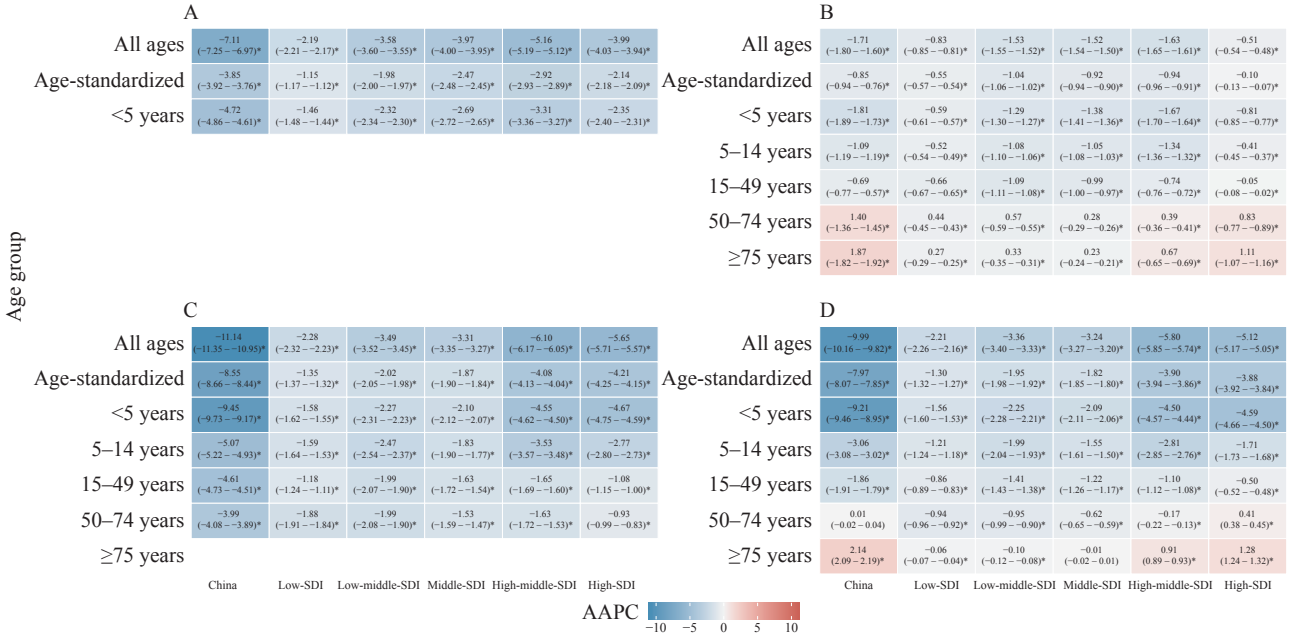

FIGURE 2. AAPCs (95% *UI*) in incidence, prevalence, mortality, and DALY rates of NTDs by age group for China and five SDI quintiles, 1990–2023. (A) Incidence; (B) Prevalence; (C) Mortality; and (D) DALYs.
Abbreviation: AAPCs=average annual percentage changes; *UI*=uncertainty interval; DALY=disability-adjusted life year; NTDs=neural tube defects; SDI=sociodemographic index.
* $P<0.05$.

SDI regions, and among those aged 75 years and older in high-middle-SDI regions.

DISCUSSION

The burden of NTDs in China declined substantially, reflecting improved prevention and control (*2*). Regional surveillance data support this trend; from 1993 to 1996, folic acid use reduced spina bifida by 78% in northern China and by 51% in southern China (*6*). China's greater decline relative to the SDI quintiles may reflect the early and sustained implementation of nationwide folic acid interventions and advances in maternal and neonatal care. However, the age-standardized prevalence rates in China rebounded from 2005 to 2023, indicating a recent reversal of the previous decline. This rebound may reflect improved survival, expanded surveillance, and greater diagnostic capacity and healthcare access, increasing the detection of individuals with NTDs, including those with associated Chiari II malformations and hydrocephalus (*1*,*7*).

Higher SDI was associated with lower age-standardized incidence, mortality, and DALY rates and steeper declines in these measures. A companion GBD 2021 analysis of congenital birth defects similarly found that mortality and DALY rates in children were negatively correlated with SDI and declined most rapidly in high- and high-middle-SDI regions, where high-quality perinatal care, folic acid fortification, and organized surveillance are more widespread (*8*). High-SDI regions also tend to report higher or rising birth prevalence than some middle-SDI regions, resulting in a U-shaped relationship between prevalence and SDI (*8*). The rising age-standardized prevalence in high-SDI regions and China may reflect improved case identification and longer survival rather than a reversal of gains in primary prevention.

The burden of NTDs is shifting toward older age groups, particularly in higher SDI regions. A 50-year Swedish register study documented a decline in birth prevalence from 5.2 to 1.2 per 10,000 births and an improvement in first-year survival from 75 to 94%, with stable mortality thereafter, resulting in an accumulating adult population over successive decades (*9*). Adult cohorts indicate that many people with spina bifida are now middle-aged or older and often have complex multisystem morbidity (*10*). This demographic shift underscores the need to strengthen life-course care pathways and long-term rehabilitation among older people with NTDs.

This study has some limitations. First, the study relies on modeled estimates from GBD 2023, which

are subject to inherent uncertainty, especially in low-SDI regions, where surveillance systems and vital registration data remain limited. Second, the GBD estimates do not include information on prenatal diagnosis or pregnancy termination, making it difficult to distinguish between true epidemiological changes and those resulting from changes in case ascertainment and reporting. Finally, the ecological framework of this study cannot fully explain the recent increases in age-standardized incidence and prevalence rates.

In conclusion, although the NTD burden in China has declined substantially since 1990, prevalence has recently increased and the burden has shifted toward older age groups, with a similar pattern observed in high-SDI regions. This shift highlights the need to integrate life-course care and rehabilitation with existing prevention strategies to reduce long-term disability among the growing population of older people with NTDs.

Conflicts of interest: No conflicts of interest.

Acknowledgements: The authors thank the Global Burden of Diseases, Injuries, and Risk Factors Study 2023 (GBD 2023) collaborators for generating and maintaining the comprehensive data resources used in this study. We are also grateful to the Institute for Health Metrics and Evaluation (IHME) for providing the GBD 2023 data.

Ethics approval and consent to participate: This study was a secondary analysis of publicly available data from the Global Burden of Disease Study 2023 (GBD 2023) database. Because the data were anonymized and did not involve direct interactions with human participants, ethical approval and informed consent were not required for this study.

Funding: National Key Research and Development Program, Ministry of Science and Technology of the People's Republic of China (2025YFC2511501); Key Project of the National Natural Science Foundation of China Regional Innovation and Development Joint Fund, National Natural Science Foundation of China (U23A20420).

doi: 10.46234/ccdcw2026.192

[#] Corresponding authors: Jufen Liu, liujufen@bjmu.edu.cn; Zhiyong Zou, harveyzou2002@bjmu.edu.cn.

[1] Institute of Reproductive and Child Health/National Health Commission Key Laboratory of Reproductive Health, Peking University, Beijing, China; [2] Department of Epidemiology and Biostatistics, School of Public Health, Peking University, Beijing, China; [3] State Key Laboratory of Female Fertility Promotion, Peking University, Beijing, China; [4] Institute of Child and Adolescent Health, School of Public Health, Peking University, National Health Commission Key Laboratory of Reproductive Health, Beijing, China.

Copyright © 2026 by Chinese Center for Disease Control and Prevention & Chinese Academy of Preventive Medicine. All content is distributed under a Creative Commons Attribution Non Commercial License 4.0 (CC BY-NC).

Submitted: August 10, 2026
Accepted: August 25, 2026
Issued: September 18, 2026

REFERENCES

1. Bai ZH, Han JR, An J, Wang H, Du XY, Yang ZC, et al. The global, regional, and national patterns of change in the burden of congenital birth defects, 1990-2021: an analysis of the global burden of disease study 2021 and forecast to 2040. eClinicalMedicine 2024;77:102873. https://doi.org/10.1016/j.eclinm.2024.102873.
2. Li WY, Chen ZY, Xu WL, Gao YY, Liu Z, Li Q, et al. Temporal trends in the prevalence of major birth defects in China: a nationwide population-based study from 2007 to 2021. World J Pediatr 2024;20(11):1145 – 54. https://doi.org/10.1007/s12519-024-00844-9.
3. Duan JC, Ding RY, Yu YB, Li ML, Ruan YP, Hu YF, et al. Global and regional burden of congenital birth defects, 1990-2021: persistent healthcare disparities and emerging challenges from non-fatal health burden. BMJ Public Health 2025;3(1):e001608. https://doi.org/10.1136/bmjph-2024-001608.
4. Bershadsky J, Riley C, Pettingell SL, Larson SA, Hall-Lande J, Hallas L, et al. Prevalence of spina bifida across the lifespan in the USA. Dev Med Child Neurol 2026;68(9):1246 – 1252 https://doi.org/10.1111/dmcn.70161.
5. GBD 2023 Demographics Collaborators. Global age-sex-specific all-cause mortality and life expectancy estimates for 204 countries and territories and 660 subnational locations, 1950-2023: a demographic analysis for the Global Burden of Disease Study 2023. Lancet 2025;406(10513):1731 – 810. https://doi.org/10.1016/s0140-6736(25)01330-3.
6. Zhou Y, Crider KS, Yeung LF, Rose CE, Li Z, Berry RJ, et al. Periconceptional folic acid use prevents both rare and common neural tube defects in China. Birth Defects Res 2022;114(5-6):184 – 96. https://doi.org/10.1002/bdr2.1983.
7. Upasani VV, Ketwaroo PD, Estroff JA, Warf BC, Emans JB, Glotzbecker MP. Prenatal diagnosis and assessment of congenital spinal anomalies: review for prenatal counseling. World J Orthop 2016;7(7):406 – 17. https://doi.org/10.5312/wjo.v7.i7.406.
8. Li YY, He C, Yu HJ, Wu D, Liu L, Zhang XY. Global, regional, and national epidemiology of congenital birth defects in children from 1990 to 2021: a cross-sectional study. BMC Pregnancy Childbirth 2025;25(1):484. https://doi.org/10.1186/s12884-025-07612-1.
9. Andersson M, Hadi L, Dellenmark Blom M, Sillen U, Sjöström S, Arnell MVM, et al. Mortality rates, cause and risk factors in people with spina bifida, register-based study over five decades. Acta Paediatr 2024;113(8):1916 – 26. https://doi.org/10.1111/apa.17275.
10. Bendt M, Gabrielsson H, Riedel D, Hagman G, Hultling C, Franzén E, et al. Adults with spina bifida: a cross-sectional study of health issues and living conditions. Brain Behav 2020;10(8):e01736. https://doi.org/10.1002/brb3.1736.

SUPPLEMENTARY MATERIALS

Disease definitions

Neural tube defects (NTDs) were defined using International Classification of Diseases, Tenth Revision (ICD-10) codes Q00-Q01.9 and Q05-Q05.9 and International Classification of Diseases, Ninth Revision (ICD-9) codes 740-741.9 and 742.0.

Age standardization

Age-standardized rates were obtained from GBD 2023 and calculated using the GBD world standard population. Beginning with GBD 2017, the standard population was updated using the unweighted mean of the age-specific proportional population distributions of national locations with populations greater than 5 million in each GBD year.

SUPPLEMENTARY TABLE S1. Examples of countries or territories by SDI quintile and SDI index value in 2023.

SDI quintile	Location name	2023 SDI index value
Low-SDI	Afghanistan	0.3337
	Angola	0.4991
	Bangladesh	0.5171
	Chad	0.2393
	Democratic Republic of the Congo	0.3950
	Haiti	0.4638
	Mozambique	0.3417
	Niger	0.2030
	Uganda	0.4421
	Yemen	0.4464
Low-middle-SDI	Belize	0.6285
	Democratic People's Republic of Korea	0.5771
	Ghana	0.5737
	Guatemala	0.5538
	Morocco	0.6124
	Myanmar	0.5320
	Namibia	0.6195
	Samoa	0.6045
	Syrian Arab Republic	0.5887
	Tajikistan	0.5512
Middle-SDI	Algeria	0.6578
	Bolivia (Plurinational State of)	0.6317
	Egypt	0.6765
	Gabon	0.6309
	Maldives	0.6610
	Mongolia	0.6597
	Palestine	0.6380
	Paraguay	0.6741
	Tonga	0.6360
	Viet Nam	0.6430

Continued

SDI quintile	Location name	2023 SDI index value
High-middle-SDI	Albania	0.7068
	Armenia	0.7173
	Azerbaijan	0.7053
	Botswana	0.6776
	Colombia	0.6888
	Costa Rica	0.7154
	Cuba	0.6949
	Fiji	0.6864
	Thailand	0.6872
	Turkmenistan	0.6822
High-SDI	Argentina	0.7647
	Australia	0.8529
	Canada	0.8873
	Germany	0.8786
	Kazakhstan	0.7272
	Lebanon	0.7237
	Malaysia	0.7704
	Republic of Korea	0.8917
	Saudi Arabia	0.8284
	Switzerland	0.9461
Not assigned	Brazil	0.6839
	China *	0.7275
	Ethiopia	0.3937
	India	0.6070
	Indonesia	0.6657
	Iran (Islamic Republic of)	0.7176
	Japan	0.8759
	Nigeria	0.5119
	Russian Federation	0.8225
	United States of America	0.8765

Abbreviation: SDI=sociodemographic index.

* China's SDI index value is 0.7275 in 2023, which falls within the high-SDI range according to the official GBD 2023 quintile cut-off.

Statistical Analysis

For absolute numbers of incident cases, prevalent cases, deaths, and DALYs, the percentage change from 1990 to 2023 was calculated as: $\frac{V_{2023} - V_{1990}}{V_{1990}} \times 100\%$, where V_{1990} and V_{2023} denote the values in 1990 and 2023, respectively. The corresponding 95% uncertainty intervals (*UI*s) were estimated using the delta method.

For the rate of each indicator, the overall temporal trend was assessed using the estimated annual percentage change (EAPC). The following log-linear model was fitted: $ln(R_t) = \alpha + \beta t + \varepsilon_t$, where R_t is the rate in year t, α is the intercept, β is the annual slope, and ε_t is the error term. The EAPC was calculated as: $EAPC = [exp(\beta) - 1] \times 100$. The 95% *UI* for the EAPC was derived from the fitted log-linear model.

Joinpoint regression was used to identify changes in trend slope. For each identified segment (k), the annual percentage change (APC) was calculated as: $APC_k = [exp(\beta_k) - 1] \times 100$. The where β_k is the slope coefficient for segment k. The average annual percentage change (AAPC) for 1990–2023 was calculated as the duration-weighted

SUPPLEMENTARY TABLE S2. Burden of NTDs in China by sex, 1990–2023.

Indicator	Group	Absolute number† (95% *UI*)			Age-standardized rates/100,000 (95% *UI*)		
		1990	2023	Percentage change (%)	1990	2023	EAPC
Incidence	Total	28,967.67 (23,124.54, 34,854.15)	3,258.36 (2,842.75, 3,694.51)	−88.75 (−88.78, −88.72)	2.66 (2.12, 3.20)	0.73 (0.64, 0.83)	−4.17 (−4.81, −3.52)*
	Male	16,144.06 (12,863.04, 19,730.37)	1,679.17 (1,463.42, 1,896.83)	−89.60 (−89.62, −89.57)	2.79 (2.22, 3.41)	0.70 (0.61, 0.80)	−4.49 (−5.13, −3.85)*
	Female	12,823.61 (10,146.78, 15,518.55)	1,579.20 (1,377.11, 17,94.04)	−87.69 (−87.72, −87.65)	2.51 (1.99, 3.04)	0.76 (0.67, 0.87)	−3.79 (−4.42, −3.14)*
Prevalence	Total	108,818.21 (83,544.31, 139,848.11)	71,879.03 (59,349.41, 86,825.24)	−33.95 (−34.16, −33.73)	9.01 (6.91, 11.56)	6.65 (5.49, 7.98)	0.11 (−0.49, 0.72)
	Male	57,047.72 (43,884.85, 72,368.86)	38,752.15 (32,111.89, 46,629.93)	−32.07 (−32.28, −31.86)	9.08 (6.99, 11.54)	6.79 (5.57, 8.20)	0.06 (−0.48, 0.60)
	Female	51,770.49 (39,322.21, 66,986.88)	33,126.88 (27,072.38, 40,038.84)	−36.01 (−36.22, −35.80)	8.95 (6.80, 11.57)	6.50 (5.35, 7.77)	0.17 (−0.52, 0.87)
Mortality	Total	15,262.52 (8,072.40, 24,418.03)	411.22 (284.88, 570.67)	−97.31 (−97.32, −97.29)	1.40 (0.74, 2.24)	0.08 (0.05, 0.11)	−10.61 (-11.48, −9.73)*
	Male	8,863.77 (4,224.18, 17,072.26)	192.16 (104.76, 297.62)	−97.83 (−97.85, −97.81)	1.53 (0.73, 2.95)	0.06 (0.03, 0.10)	−11.69 (-12.64, −10.74)*
	Female	6,398.75 (3,034.62, 11,323.23)	219.06 (128.45, 350.43)	−96.58 (−96.60, −96.55)	1.25 (0.59, 2.21)	0.09 (0.05, 0.15)	−9.47 (−10.28, −8.65)*
DALYs	Total	1,395,231.49 (764,333.07, 2,213,112.98)	55,780.00 (41,672.03, 71,605.38)	−96.00 (−96.03, −95.98)	127.44 (69.40, 202.51)	8.58 (6.20, 11.57)	−9.96 (−10.76, −9.15)*
	Male	808,850.10 (393,333.73, 1,542,350.56)	27,283.96 (18,826.78, 37,223.41)	−96.63 (−96.65, −96.60)	139.37 (67.66, 266.18)	7.33 (4.73, 10.92)	-10.89 (-11.75, −10.02)*
	Female	586,381.39 (280,458.44, 1,025,532.93)	28,496.04 (19,893.00, 40,242.06)	−95.14 (−95.18, −95.10)	113.95 (54.33, 199.80)	10.03 (6.21, 15.35)	−8.94 (−9.69, −8.18)*

Abbreviation: NTDs=neural tube defects; EAPC=estimated annual percentage change; *UI*=uncertainty interval; DALYs=disability-adjusted life years.

* $P<0.05$.

† Absolute numbers represent incident cases, prevalent cases, deaths, and total DALYs, whereas rates represent incidence, prevalence, mortality, and DALY rates.

geometric mean of the segment-specific APCs: $AAPC = \left\{ exp\left[\frac{\sum_{k=1}^{K} w_k \beta_k}{\sum_{k=1}^{K} w_k} \right] - 1 \right\} \times 100$, where K is the total number of identified segments and w_k is the duration, in years, of segment k.

SUPPLEMENTARY TABLE S3. Burden of NTDs in China by age group, 1990–2023.

Indicator	Age group (years)	Absolute number[†] (95% *UI*)			Age-specific rates/100,000 (95% *UI*)		
		1990	2023	Percentage change (%)	1990	2023	EAPC
Incidence	<5	28,967.67 (23,124.54, 34,854.15)	3,258.36 (2,842.75, 3,694.51)	−88.75 (−88.78, −88.72)	26.13 (20.86, 31.44)	5.24 (4.57, 5.94)	−4.70 (−5.15, −4.24)*
Prevalence	<5	33,636.61 (25,902.89, 42,673.17)	10,078.06 (8,279.60, 12,053.12)	−70.04 (−70.13, −69.95)	30.35 (23.37, 38.50)	16.21 (13.32, 19.39)	−0.72 (−1.51, 0.07)
	5–14	31,183.63 (23,648.15, 39,957.52)	19,372.22 (16,052.01, 23,345.94)	−37.88 (−38.08, −37.68)	15.06 (11.42, 19.29)	10.20 (8.45, 12.29)	−0.04 (−0.74, 0.67)
	15–49	41,291.46 (30,730.95, 54,380.37)	30,728.30 (25,245.62, 37,301.22)	−25.58 (−25.84, −25.32)	6.18 (4.60, 8.13)	4.76 (3.91, 5.78)	0.12 (−0.37, 0.61)
	50–74	2,497.05 (1,645.49, 3,568.67)	10,182.51 (7,810.44, 12,835.11)	307.78 (305.92, 309.65)	1.44 (0.95, 2.06)	2.24 (1.72, 2.82)	1.96 (1.67, 2.25)*
	≥75	209.46 (134.61, 311.92)	1,517.95 (1,149.60, 1,897.09)	624.68 (621.13, 628.23)	1.08 (0.69, 1.60)	1.96 (1.48, 2.45)	2.43 (2.14, 2.73)*
Mortality	<5	14,916.00 (7,820.86, 24,030.19)	341.41 (210.54, 496.61)	−97.71 (−97.73, −97.70)	13.46 (7.06, 21.68)	0.55 (0.34, 0.80)	−11.10 (−12.05, −10.12)*
	5–14	199.17 (116.75, 315.83)	32.80 (22.25, 49.17)	−83.53 (−83.64, −83.43)	0.10 (0.06, 0.15)	0.02 (0.01, 0.03)	−5.86 (−6.12, −5.60)*
	15–49	130.63 (75.64, 193.88)	26.38 (17.86, 39.58)	−79.80 (−79.93, −79.68)	0.020 (0.011, 0.029)[§]	0.004 (0.003, 0.006)	−5.29 (−5.68, −4.90)*
	50–74	16.72 (9.51, 26.43)	10.63 (6.80, 14.77)	−36.43 (−36.83, −36.03)	0.010 (0.005, 0.015)	0.002 (0.001, 0.003)	−4.42 (−4.67, −4.17)*
DALYs	<5	1,348,257.20 (711,574.19, 2,166,384.41)	33,430.03 (21,826.13, 47,022.07)	−97.52 (−97.54, −97.50)	1216.36 (641.96, 1954.45)	53.78 (35.11, 75.64)	−10.87 (-11.80, −9.94)*
	5–14	25,495.80 (17,369.37, 35,496.53)	8,508.12 (6,376.62, 10,960.37)	−66.63 (−66.78, −66.48)	12.31 (8.39, 17.14)	4.48 (3.36, 5.77)	−3.12 (−3.43, −2.82)*
	15–49	20,281.54 (14,292.24, 26,933.17)	10,461.86 (7,505.61, 13,864.44)	−48.42 (−48.64, −48.19)	3.03 (2.14, 4.03)	1.62 (1.16, 2.15)	−1.54 (−1.81, −1.26)*
	50–74	1,147.75 (790.06, 1,546.95)	2,989.48 (2,144.37, 4,084.64)	160.46 (159.26, 161.67)	0.66 (0.46, 0.89)	0.66 (0.47, 0.90)	0.42 (0.24, 0.60)*
	≥75	49.20 (29.57, 76.00)	390.51 (255.36, 569.68)	693.74 (688.81, 698.66)	0.25 (0.15, 0.39)	0.50 (0.33, 0.74)	2.87 (2.52, 3.22)*

Abbreviation: NTDs=neural tube defects; EAPC=estimated annual percentage change; *UI*=uncertainty interval; DALYs=disability-adjusted life years.

* $P<0.05$.

[†] Absolute numbers represent incident cases, prevalent cases, deaths, and total DALYs, whereas rates represent incidence, prevalence, mortality, and DALY rates.

[§] The four small nonzero estimates shown to three decimal places are reported at this precision to avoid rounding to zero; all other values are reported to two decimal places.

Preplanned Studies

Associations Between Longitudinal Antenatal Hematological Indicators and Risk of Patent Ductus Arteriosus in Newborns — Beijing, China, 2011–2025

Xiaoqian Jia[1,2,3,&]; Pengbo Yuan[4,&]; Jufen Liu[1,2,3]; Zhiwen Li[1,2,3]; Yuan Wei[4,#]; Tianchen Wu[1,3,#]

Summary

What is already known about this topic?

Patent ductus arteriosus (PDA) is closely associated with prematurity. Maternal conditions may increase offspring cardiac risk. However, antenatal hematological evidence remains limited.

What is added by this report?

Among 68,945 singleton live births, 945 were diagnosed with PDA. After false discovery rate correction, trimester-specific indicators, particularly prothrombin time and thrombin time, were found to be associated with PDA risk. The patterns differed by preterm birth, hypertensive disorders of pregnancy, gestational diabetes mellitus, and conception mode.

What are the implications for public health practice?

Routine maternal hematological indicators may provide preliminary evidence for further investigation of perinatal risk markers and may help identify pregnancies and newborns who may benefit from closer cardiovascular surveillance.

ABSTRACT

Introduction: This study aimed to examine whether longitudinal antenatal hematological indicators are associated with the risk of patent ductus arteriosus (PDA) in neonates.

Methods: A retrospective cohort study was conducted using electronic medical records from the Peking University Third Hospital, including 68,945 singleton live births between December 2011 and June 2025. Routine prenatal hematological, inflammatory, and coagulation-related indicators were summarized by trimester and standardized before analysis. Logistic regression models were used to estimate adjusted odds ratios (*OR*s) for PDA per 1-SD increase in each indicator, with false discovery rate correction (FDR) for multiple testing. Stratified analyses were conducted by preterm birth, hypertensive disorders of pregnancy, gestational diabetes mellitus, and conception mode.

Results: Among 68,945 neonates, 945 (1.37%) were diagnosed with PDA. The preterm birth rate (61.69% *vs*. 8.12%) and NICU (Neonatal intensive care unit) admission rate (80.11% *vs*. 4.47%) were higher in the PDA group than in the non-PDA group. After FDR correction, longitudinal antenatal hematological profiles differed between neonates with and without PDA, with mean platelet volume (MPV) consistently and activated partial thromboplastin time (APTT) inversely associated with PDA across gestation. In the third trimester, each 1-SD increase in MPV and prothrombin time (PT) was associated with higher odds of PDA {adjusted *OR*s of 1.12 [95% confidence interval (*CI*): 1.05–1.20] and 1.25 (95% *CI*: 1.19–1.31), respectively}, whereas each 1-SD increase in APTT was associated with lower odds (adjusted *OR*, 0.81; 95% *CI*: 0.75–0.88).

Conclusion: Trimester-specific prenatal hematological indicators were associated with neonatal PDA risk, with distinct patterns between term and preterm births and across maternal subgroups. Routinely collected antenatal laboratory data may help characterize PDA-related perinatal risk and warrant further evaluation in future risk prediction research.

Patent ductus arteriosus (PDA) is a common cardiovascular condition in neonates and represents an important adverse outcome within the spectrum of congenital heart disease, particularly among preterm infants (*1–4*). Although prematurity is the dominant risk factor, maternal hypertensive disorders, diabetes, and the use of assisted reproductive technologies (ART) have also been associated with an increased cardiac risk (*4–7*). Routine prenatal hematological indicators may reflect maternal inflammatory, hemostatic, and metabolic status. However, their

Copyright © 2026 by Chinese Center for Disease Control and Prevention

interpretation requires consideration of physiological changes during gestation (*8*).

Evidence remains limited regarding whether longitudinal antenatal hematological indicators are associated with neonatal PDA risk. Therefore, this study assessed trimester-specific associations between routinely measured prenatal hematological, inflammatory, and coagulation-related indicators and neonatal PDA using stratified analyses by preterm birth, hypertensive disorders of pregnancy (HDP), gestational diabetes mellitus (GDM), and conception mode.

This retrospective cohort study used electronic medical record data from the Peking University Third Hospital. Singleton pregnancies resulting in live births between December 2011 and June 2025 were eligible for inclusion. Maternal prenatal laboratory results, obstetric characteristics, disease diagnoses, delivery information, and neonatal outcomes were obtained from the hospital information system. All diagnoses were identified from medical records using the ICD-10 codes, with PDA identified using code Q25.001. The primary outcome was the occurrence of PDA among live-born infants. Maternal blood tests were treated as longitudinal measurements, and each participant underwent at least three blood examinations during pregnancy at early, mid, and late gestation. The Peking University Third Hospital Medical Science Research Ethics Committee approved this study (IRB00006761-M20250060).

Maternal hematological exposures included complete blood count markers, coagulation-related markers, and inflammatory markers measured during pregnancy. Hematology results were linked to gestational age at sampling and categorized as first trimester (≤12 weeks), second trimester (13–27 weeks), and third trimester (≥28 weeks). For trimester-specific analyses, repeated measurements within the same trimester were summarized using the within-person median for each marker. These trimester-specific marker values were standardized prior to modeling.

Potential confounders included pre-pregnancy body mass index (BMI), gestational weight gain, maternal age, parity, ART, gestational age at delivery, HDP, and GDM. Pregnancy and neonatal outcomes were compared between the PDA and non-PDA groups, including delivery method, gestational age at delivery, preterm birth (<37 weeks), birth weight, birth length, infant sex, neonatal intensive care unit (NICU) admission, and respiratory distress syndrome, and were further classified as small-for-gestational-age, appropriate-for-gestational-age, or large-for-gestational-age based on Chinese reference standards (*9*).

Categorical variables were summarized as numbers and percentages and compared using Pearson's chi-square test. Normally distributed continuous variables were presented as means and standard deviations and compared using *t*-test, whereas non-normally distributed variables were presented as medians and interquartile ranges and compared using the Wilcoxon rank-sum test. To characterize longitudinal changes in maternal blood parameters across gestation, mixed-effects models with restricted cubic splines for gestational age were fitted for each biomarker, with participant-level random effects used to account for repeated measurements. Differences in trajectories between the PDA and non-PDA groups were evaluated using likelihood ratio tests. To quantify the associations during clinically relevant periods, logistic regression models were fitted separately for the first, second, and third trimesters. For each marker, the results were reported as adjusted odds ratios (*OR*s) and 95% confidence intervals (*CI*s) per 1-SD increase, with each marker being standardized before regression analysis by subtracting its mean and dividing by its standard deviation in the analytic sample. Multivariable models were adjusted for the confounders listed above. Stratified analyses were performed within strata defined by preterm birth, HDP, GDM, and use of ART. As multiple markers were tested, false discovery rate (FDR) correction was applied to analyses across all tested hematological indicators within the three trimesters. All statistical analyses were performed using SAS (version 9.4, SAS Institute Inc., Cary, NC, USA) and R (version 4.5.2, R Foundation for Statistical Computing, Vienna, Austria). All tests were two-sided, and a P value <0.05 was considered statistically significant.

As shown in Table 1, among 68,945 eligible participants, 945 neonates were diagnosed with PDA (1.37%) and 68,000 served as controls. Compared with controls, neonates with PDA were more often born to mothers with higher pre-pregnancy BMI [23.12±3.67 *vs.* 22.06±3.28], lower gestational weight gain [11.39±4.89 *vs.* 12.90±4.49], and older maternal age [33.80±4.17 *vs.* 33.09±3.93 years, all P<0.01]. Advanced maternal age, multiparity, and ART conception were also more frequent in the PDA group than in controls [37.99% (359/945) *vs.* 30.59% (20,803/68,000); 36.72% (347/945) *vs.* 26.91% (18,301/68,000); and 13.86% (131/945) *vs.* 11.31%

TABLE 1. Comparison of baseline characteristics between groups.

Characteristics	All (*N*=68,945)	PDA group, *n* (%) (*N*=945)	Non-PDA group, *n* (%) (*N*=68,000)	*P*
Pre-pregnancy BMI (kg/m^2)	22.08±3.29	23.12±3.67	22.06±3.28	<0.01*
Gestational weight gain (kg)	12.88±4.50	11.39±4.89	12.90±4.49	<0.01*
Maternal age (years)	33.10±3.93	33.80±4.17	33.09±3.93	<0.01*
Advanced maternal age				
No	47,783	586 (62.01)	47,197 (69.41)	<0.01†
Yes	21,162	359 (37.99)	20,803 (30.59)	
Parity				
Primipara	50,297	598 (63.28)	49,699 (73.09)	<0.01†
Multipara	18,648	347 (36.72)	18,301 (26.91)	
Assisted reproductive technology				
No	61,125	814 (86.14)	60,311 (88.69)	0.01†
Yes	7,820	131 (13.86)	7,689 (11.31)	
Hypertensive disorders of pregnancy				
No	61,092	637 (67.41)	60,455 (88.9)	<0.01†
Yes	7,853	308 (32.59)	7,545 (11.10)	
Preeclampsia				
No	64,738	695 (73.54)	64,043 (94.18)	<0.01†
Yes	4,207	250 (26.46)	3,957 (5.82)	
Gestational diabetes mellitus				
No	52,570	679 (71.85)	51,891 (76.31)	<0.01†
Yes	16,375	266 (28.15)	16,109 (23.69)	
Delivery method				
Cesarean delivery	28,551	612 (64.76)	27,939 (41.09)	<0.01†
Vaginal delivery	40,394	333 (35.24)	40,061 (58.91)	
Gestational age at delivery (week)	38.93±1.93	35.12±3.78	38.98±1.84	<0.01*
Preterm birth				
No	62,843	362 (38.31)	62,481 (91.88)	<0.01†
Yes	6,102	583 (61.69)	5,519 (8.12)	
Birth weight (g)	3,231.55±526.19	2,412.23±912.36	3,242.94±509.62	<0.01*
Appropriate for gestational age	55,055	685 (72.49)	54,370 (79.96)	<0.01†
Large for gestational age	9,540	156 (16.51)	9,384 (13.8)	
Small for gestational age	4,350	104 (11.01)	4,246 (6.24)	
Birth length (cm)	49.14±2.58	44.74±5.17	49.20±2.47	<0.01*
Gender				
Boys	35,782	487 (51.53)	35,295 (51.9)	0.82†
Girls	33,163	458 (48.47)	32,705 (48.1)	
NICU admission				
No	65,147	188 (19.89)	64,959 (95.53)	<0.01†
Yes	3,798	757 (80.11)	3,041 (4.47)	
Respiratory distress syndrome				
No	68,177	572 (60.53)	67,605 (99.42)	<0.01†
Yes	768	373 (39.47)	395 (0.58)	

Abbreviation: BMI=body mass index; NICU=neonatal intensive care unit; PDA=patent ductus arteriosus.
* Continuous variables are presented as means and standard deviations, and between-group differences were assessed using *t*-tests.
† Categorical variables are presented as numbers and percentages, and between-group differences were assessed using Pearson chi-square tests.

(7,689/68,000), respectively]. Pregnancy complications were more frequent in mothers of neonates with PDA than in controls. HDP occurred in 32.59% (308/945) *vs.* 11.10% (7,545/68,000, *P*<0.01), and preeclampsia in 26.46% (250/945) *vs.* 5.82% (3,957/68,000, *P*<0.01). GDM was also higher in the PDA group [28.15% (266/945) *vs.* 23.69% (16,109/68,000), *P*<0.01]. Compared with controls, neonates with PDA had a lower gestational age at delivery, lower birth weight, higher rates of preterm birth and cesarean delivery, greater proportions of small- and large-for-gestational-age infants, while the distribution of fetal

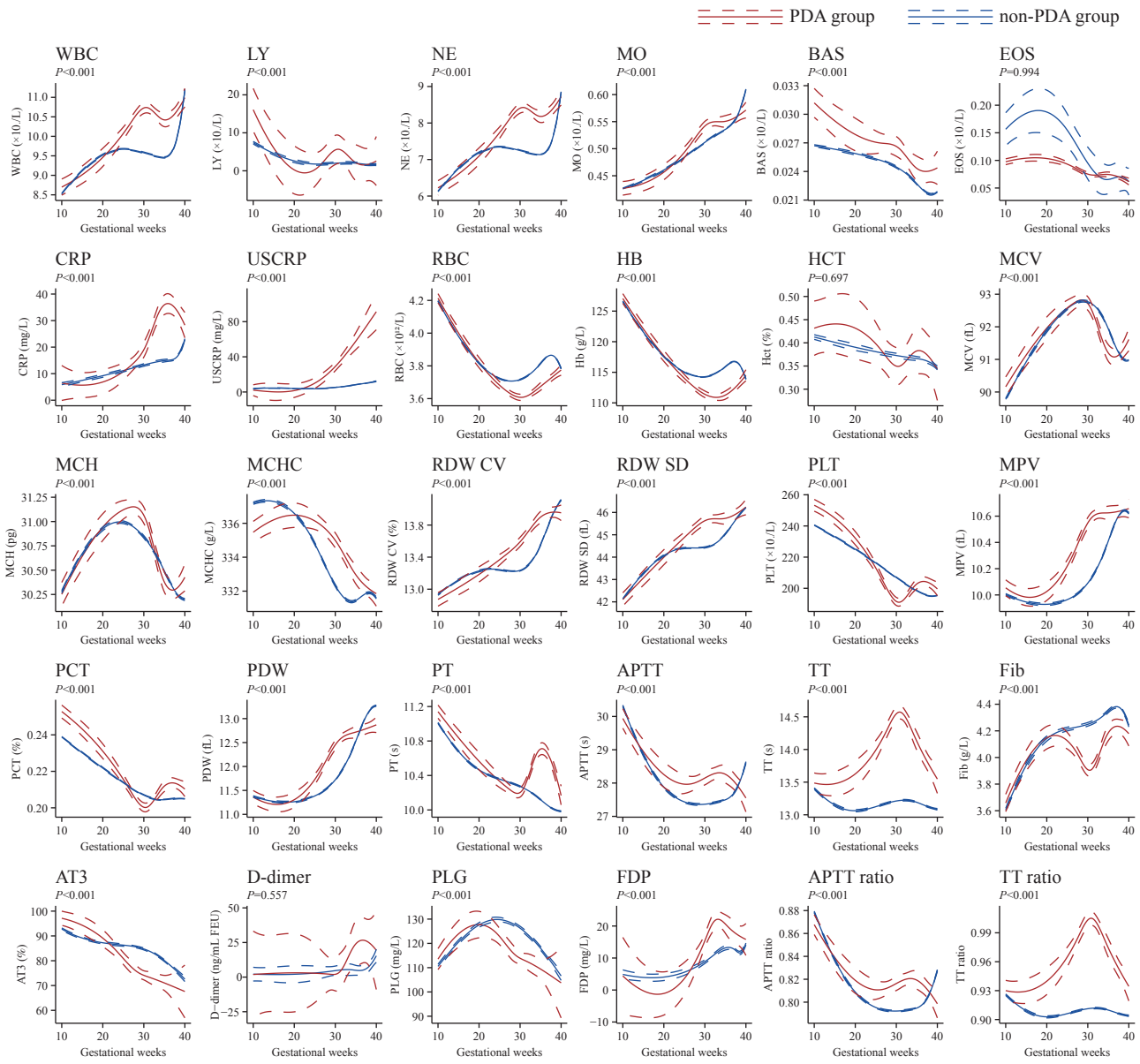

FIGURE 1. Comparison of hematologic test trajectories between the PDA and non-PDA groups.
Note: *P* values indicate FDR-adjusted *P*-values.
Abbreviation: WBC=white blood cell; LY=lymphocyte; NE=neutrophil; MO=monocyte; BAS=basophil; EOS=eosinophil; CRP=C-reactive protein; USCRP=Ultra-sensitive C-reactive protein; RBC=red blood cell; HB=hemoglobin; HCT=hematocrit; MCV=mean corpuscular volume; MCH=mean corpuscular hemoglobin; MCHC=mean corpuscular hemoglobin concentration; RDW CV=red cell distribution width coefficient of variation; RDW SD=red cell distribution width standard deviation; PLT=platelet; MPV=mean platelet volume; PCT=plateletcrit; PDW=platelet distribution width; PT=prothrombin time; APTT=activated partial thromboplastin time; TT=thrombin time; Fib=fibrinogen; AT3=antithrombin III; PLG=plasminogen; FDP=fibrin degradation products; APTT ratio=activated partial thromboplastin time ratio; TT ratio=thrombin time ratio.

sex was similar between groups. They also showed higher rates of NICU admission and respiratory distress syndrome.

As shown in Figure 1, most indicators showed significantly different pregnancy trajectories between the PDA and non-PDA groups after FDR correction, including white blood cell count and differentials[*] (WBC, LY, NE, MO, and BAS), red-cell indices[†] (RBC, HB, MCV, MCH, MCHC, RDW CV, and RDW SD), platelet indices[§] (PLT, MPV, PCT, and PDW), coagulation-related markers[¶] (PT, APTT, TT, Fib, AT3, PLG, FDP, APTT ratio, and TT ratio), and C-Reactive Protein (CRP)/Ultra-Sensitive CRP (USCRP) (P<0.001). In contrast, eosinophil (EOS), hematocrit (HCT), and D-dimer levels did not show significant group-level trajectory differences in the supplied trajectory figure (P=0.994, P=0.697, and P=0.557, respectively).

As shown in Figure 2, after FDR correction, significant associations were concentrated in the selected coagulation-, inflammatory-, and erythrocyte-related indicators. In the overall population, higher *ORs* were observed for BAS in the first and third trimesters, MPV in all three trimesters, PT in the first and third trimesters, and TT/TT ratio in the second and third trimesters. The third-trimester CRP levels also reached significance. In contrast, lower *ORs* were observed for first-trimester MCHC; second-trimester NE, APTT, and APTT ratio; and third-trimester RBC, HB, HCT, APTT, Fib, AT3, and APTT ratio. Preterm birth stratification showed distinct patterns. Among term births, significant positive associations were mainly observed for BAS, PT, TT, and TT ratio, with additional signals for CRP and MCV, whereas inverse associations were observed for MCHC, MO, APTT, and APTT ratio. Among preterm births, significant associations were confined to the third trimester; MPV, PT, TT, and TT ratio showed higher *ORs,* whereas RBC, HB, HCT, APTT, Fib, and APTT ratio showed lower *OR*s. Among women without HDP or GDM, the pattern generally resembled that observed in the overall population, characterized by positive associations for BAS and PT/TT/TT ratio and inverse associations for APTT/APTT ratio and selected erythrocyte-related markers. Among women with HDP, significant associations were restricted to the third trimester and included the MPV, APTT, TT, FDP, APTT ratio, and TT ratio. Similarly, among women with GDM, only third-trimester associations remained significant, including higher *OR*s for MPV, PT, and TT and lower *OR*s for APTT, AT3, and APTT ratio. Natural conceptions closely mirrored the overall pattern. In assisted reproductive pregnancies, significant associations were fewer and confined to the third trimester, involving higher *OR*s for MPV, PDW, TT, and TT ratio and lower *OR*s for RBC, HB, HCT, APTT, and APTT ratio.

DISCUSSION

In this large retrospective cohort study, longitudinal antenatal hematological indicators showed trimester- and subgroup-specific associations with neonatal PDA risk. The most consistent FDR-significant findings involved coagulation markers, with PT, TT, and TT ratio generally showing positive associations, and APTT and APTT ratio showing inverse associations. MPV was positively associated with PDA across the three trimesters, whereas inverse erythrocyte-related associations, particularly for RBC, HB, and HCT, were observed mainly in late pregnancy. Subgroup analyses revealed further heterogeneity, with significant findings among preterm births. Women with HDP or GDM were largely concentrated in the third trimester. These findings suggest that routinely collected antenatal hematological profiles may provide complementary information for PDA risk assessment and targeted perinatal surveillance, although further validation is required before clinical application.

The associations of PT, TT, and TT ratio with higher PDA risk were consistently observed across the overall population and multiple strata. APTT and APTT ratio assess the intrinsic and common coagulation pathways, whereas TT and TT ratio reflect terminal fibrin formation. Thus, their opposite associations may reflect different aspects of maternal hemostasis rather than inconsistent findings. However, these maternal coagulation markers do not directly measure fetal ductal physiology, and the underlying mechanisms remain unclear. As ductal closure is

[*] WBC=white blood cell; LY=lymphocyte; NE=neutrophil; MO=monocyte; BAS=basophil.

[†] RBC=red blood cell; HB=hemoglobin; MCV=mean corpuscular volume; MCH=mean corpuscular hemoglobin; MCHC=mean corpuscular hemoglobinconcentration; RDW CV=red cell distribution width coefficient of variation; RDW SD=red cell distribution width standarddeviation.

[§] PLT=platelet; MPV=mean platelet volume; PCT=plateletcrit; PDW=platelet distribution width.

[¶] PT=prothrombintime; APTT=activated partial thromboplastin time; TT=thrombin time; Fib=Fibrinogen; AT3=antithrombin III; PLG=plasminogen; FDP=fibrin degradation products; APTT ratio=activated partial thromboplastin time ratio; TTratio=thrombin time ratio.

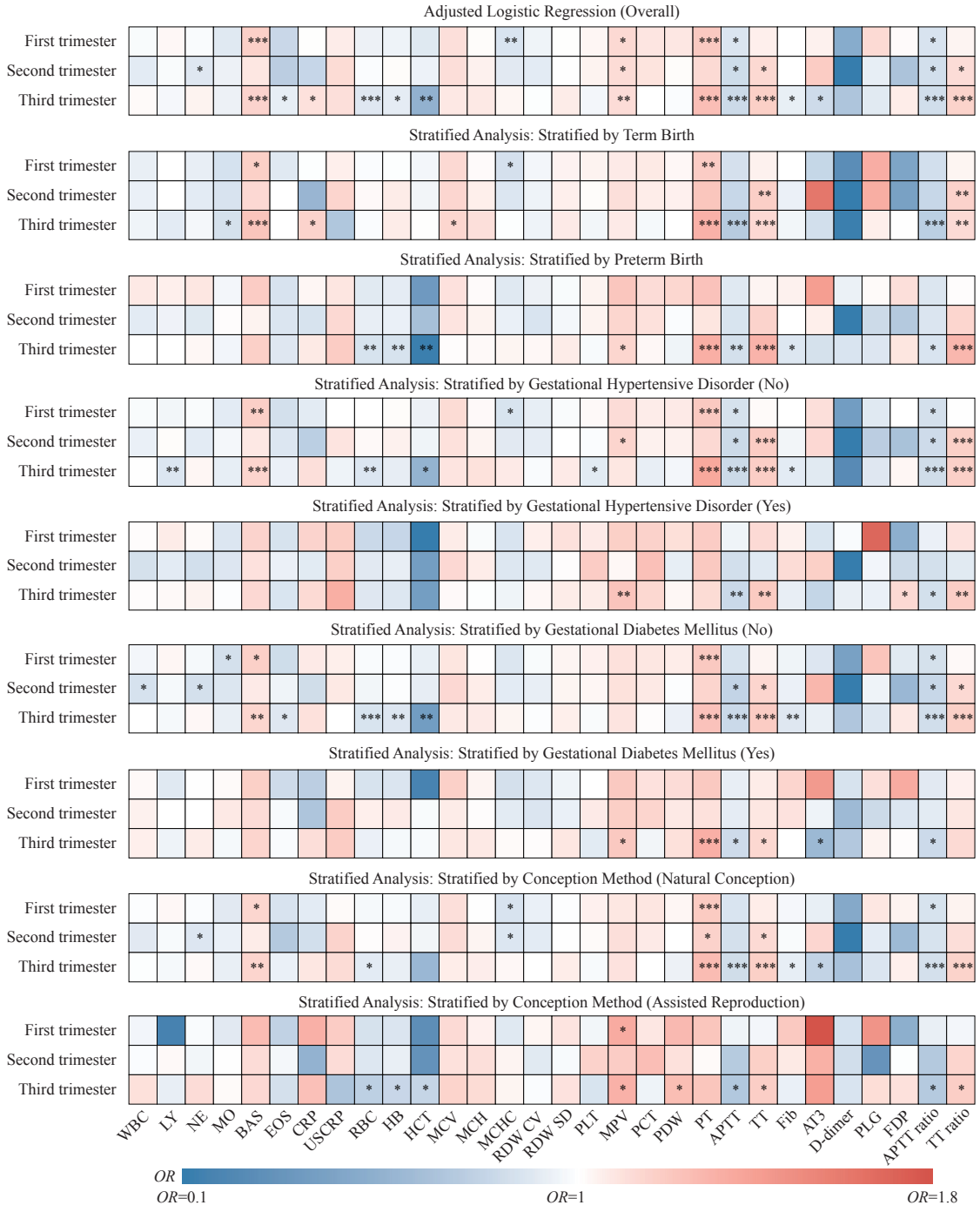

FIGURE 2. Trimester-specific associations of prenatal hematological indicators with neonatal patent ductus arteriosus risk: Overall and stratified analyses.

Note: Colors represent adjusted *OR*s on the original scale for PDA per 1-SD increase in each prenatal indicator.

Abbreviation: WBC=white blood cell; LY=lymphocyte; NE=neutrophil; MO=monocyte; BAS=basophil; EOS=eosinophil; CRP=C-reactive protein; USCRP=ultra-sensitive C-reactive protein; RBC=red blood cell; HB=hemoglobin; HCT=hematocrit; MCV=mean corpuscular volume; MCH=mean corpuscular hemoglobin; MCHC=mean corpuscular hemoglobin concentration; RDW CV=red cell distribution width coefficient of variation; RDW SD=red cell distribution width standard deviation; PLT=platelet; MPV=mean platelet volume; PCT=plateletcrit; PDW=platelet distribution width; PT=prothrombin time; APTT=activated partial thromboplastin time; TT=thrombin time; Fib=Fibrinogen; AT3=antithrombin III; PLG=plasminogen; FDP=fibrin degradation products; APTT ratio=activated partial thromboplastin time ratio; TT ratio=thrombin time ratio.

* $P<0.05$;

** $P<0.01$;

*** $P<0.001$.

regulated by oxygen tension, prostaglandins, nitric oxide, platelet activity, and vascular remodeling (*3–4*,*10*), the observed associations may reflect broader maternal conditions related to postnatal ductal adaptation.

Preterm birth stratification suggested heterogeneity, with term births showing a broader pattern across gestation, whereas associations among preterm births were confined to the third trimester. Because prematurity influences PDA and may have different roles in the causal pathway, we additionally examined models without adjustment for gestational age, which yielded similar results. In preterm births, higher coagulation- and platelet-related indicators were inversely associated with RBC, HB, and HCT levels. These findings may indicate differences by prematurity status, although residual confounding factors related to preterm birth and their causes cannot be excluded. This erythrocyte-related pattern may reflect hemodilution or altered maternal-placental-fetal oxygen transport. This interpretation is biologically plausible because oxygen tension is central to postnatal ductal constriction (*3*); however, maternal erythrocyte indices do not measure fetal oxygenation.

The inflammatory findings were selective. BAS was positively associated with PDA risk across multiple strata, whereas CRP level was significant only in the overall and term birth analyses. This selective pattern is consistent with the mixed findings of previous studies, although experimental evidence suggests that inflammatory stimulation may delay ductal closure through nitric oxide-related mechanisms (*11–13*). HDP, GDM, and ART were associated with distinct marker profiles. The findings in HDP and GDM were confined to the third trimester, whereas those in ART pregnancies were fewer and predominantly observed in late pregnancy. These differences may reflect smaller subgroup sample sizes, altered baseline laboratory distributions, or distinct vascular–metabolic profiles associated with hypertension, diabetes, and ART pregnancies (*5–7*).

This study has several strengths, including its large obstetric cohort, longitudinal prenatal laboratory data, trimester-specific modeling, FDR correction, and clinically relevant stratified analyses. However, as all data were obtained from a single hospital, the study population's medical characteristics, prenatal examination protocols, and neonatal diagnostic and treatment practices may have been center-specific, limiting the racial and regional generalizability of our findings. In addition, unmeasured clinical factors, such as infection, medication use, nutritional status, and differences in neonatal cardiac screening, may have influenced the observed associations. Future multicenter studies are needed to validate these findings and assess their generalizability.

Conflicts of interest: No conflicts of interest.

Acknowledgments: All participants were involved in the establishment and maintenance of the obstetric cohort at the Peking University Third Hospital.

Ethical statement: Approved by the Peking University Third Hospital Medical Science Research Ethics Committee (IRB00006761-M20250060).

Funding: Supported by the National Natural Science Foundation of China (Grant No. 82504425); the Key R&D Program of Tibet Autonomous Region (XZ202401ZY0042); the Beijing Administration of Traditional Chinese Medicine (BJZYZD-2025-22); the Joint Funds of Capital's Funds for Health Improvement and Research (2026-M2-4-409-2); and the Clinical Cohort Construction Program of Peking University Third Hospital (BYSYDL2026032).

doi: 10.46234/ccdcw2026.191

[#] Corresponding authors: Yuan Wei, weiyuan@bjmu.edu.cn; Tianchen Wu, wtc17@pku.edu.cn.

[1] Institute of Reproductive and Child Health/National Health Commission Key Laboratory of Reproductive Health, School of Public Health/Department of Obstetrics and Gynecology, Third Hospital, Peking University, Beijing, China; [2] Department of Epidemiology and Biostatistics, School of Public Health, Peking University, Beijing, China; [3] State Key Laboratory of Female Fertility Promotion, Peking University, Beijing, China; [4] National Centre for Healthcare Quality Management in Obstetrics, Beijing, China.
[&] Joint first authors.

Copyright © 2026 by Chinese Center for Disease Control and Prevention & Chinese Academy of Preventive Medicine. All content is distributed under a Creative Commons Attribution Non Commercial License 4.0 (CC BY-NC).

Submitted: July 17, 2026
Accepted: September 07, 2026
Issued: September 18, 2026

REFERENCES

1. van der Linde D, Konings EEM, Slager MA, Witsenburg M, Helbing WA, Takkenberg JJM, et al. Birth prevalence of congenital heart disease worldwide: a systematic review and meta-analysis. J Am Coll Cardiol 2011;58(21):2241 – 7. https://doi.org/10.1016/j.jacc.2011.08.025.
2. Liu YJ, Chen S, Zühlke L, Black GC, Choy MK, Li NX, et al. Global birth prevalence of congenital heart defects 1970-2017: updated systematic review and meta-analysis of 260 studies. Int J Epidemiol 2019;48(2):455 – 63. https://doi.org/10.1093/ije/dyz009.
3. Schneider DJ, Moore JW. Patent ductus arteriosus. Circulation 2006;114(17):1873 – 82. https://doi.org/10.1161/CIRCULATIONAHA.105.592063.
4. Hamrick SEG, Sallmon H, Rose AT, Porras D, Shelton EL, Reese J, et al. Patent ductus arteriosus of the preterm infant. Pediatrics 2020;146

(5):e20201209. https://doi.org/10.1542/peds.2020-1209.
5. Chen LT, Yang TB, Chen LZ, Wang LS, Wang TT, Zhao LJ, et al. Risk of congenital heart defects in offspring exposed to maternal diabetes mellitus: an updated systematic review and meta-analysis. Arch Gynecol Obstet 2019;300(6):1491 – 506. https://doi.org/10.1007/s00404-019-05376-6.
6. Galdini A, Fesslova VME, Gaeta G, Candiani M, Pozzoni M, Chiarello C, et al. Prevalence of congenital heart defects in pregnancies conceived by assisted reproductive technology: a cohort study. J Clin Med 2021;10(22):5363. https://doi.org/10.3390/jcm10225363.
7. Ramakrishnan A, Lee LJ, Mitchell LE, Agopian AJ. Maternal hypertension during pregnancy and the risk of congenital heart defects in offspring: a systematic review and meta-analysis. Pediatr Cardiol 2015;36(7):1442 – 51. https://doi.org/10.1007/s00246-015-1182-9.
8. Abbassi-Ghanavati M, Greer LG, Cunningham FG. Pregnancy and laboratory studies: a reference table for clinicians. Obstet Gynecol 2009;114(6):1326 – 31. https://doi.org/10.1097/AOG.0b013e3181c2bde8.
9. Capital Institute of Pediatrics, the Coordinating Study Group of Nine Cities on the Physical Growth and Development of Children. Growth standard curves of birth weight, length and head circumference of Chinese newborns of different gestation. Chin J Pediatr 2020;58(9):738 – 46. https://doi.org/10.3760/cma.j.cn112140-20200316-00242.
10. Kajino H, Chen YQ, Chemtob S, Waleh N, Koch CJ, Clyman RI. Tissue hypoxia inhibits prostaglandin and nitric oxide production and prevents ductus arteriosus reopening. Am J Physiol Regul Integr Comp Physiol 2000;279(1):R278 – 86. https://doi.org/10.1152/ajpregu.2000.279.1.R278.
11. Behbodi E, Villamor-Martínez E, Degraeuwe PLJ, Villamor E. Chorioamnionitis appears not to be a risk factor for patent ductus arteriosus in preterm infants: a systematic review and meta-analysis. Sci Rep 2016;6(1):37967. https://doi.org/10.1038/srep37967.
12. Park HW, Choi YS, Kim KS, Kim SN. Chorioamnionitis and patent ductus arteriosus: a systematic review and meta-analysis. PLoS One 2015;10(9):e0138114. https://doi.org/10.1371/journal.pone.0138114.
13. Kajimura I, Akaike T, Minamisawa S. Lipopolysaccharide delays closure of the rat ductus arteriosus by induction of inducible nitric oxide synthase but not prostaglandin E_2. Circ J 2016;80(3):703 – 11. https://doi.org/10.1253/circj.CJ-15-1053.

Preplanned Studies

School-Based Scoliosis Screening Among Children and Adolescents — Wusu City, Xinjiang Uygur Autonomous Region, China, January 2026

Zhongcheng An[1,&]; Junwei Feng[2,&]; Tao Xu[3,&]; Zeyu Lu[1]; Muradil Mardan[1]; Bing Wu[2]; Jiayi Dou[2]; Han Zhang[2]; Jiale Zhang[2]; Weibin Sheng[3]; Lingjie Fu[1]; Feng Lin[1]; Jufen Liu[4,5]; Bo Li[1]; Yuanyuan Cao[6]; Shengdan Jiang[1]; Xiaofeng Peng[7,#]; Xinfeng Zheng[1,#]

Summary

What is already known about this topic?

School-based scoliosis screening can identify children needing further evaluation and is increasingly promoted nationally, yet real-world screening evidence from multi-ethnic populations in northwestern China remains limited.

What is added by this report?

In a real-world school screening program in Wusu City, northern Xinjiang Uygur Autonomous Region, that included 18,631 students, the artificial intelligence-assisted screen-positive rate was 5.36%, whereas the final screen-positive rate after specialist review was 2.62%. Age was the most consistent signal, with positivity highest in junior and senior high school (*P* for trend <0.001). However, only 24.59% of final screen-positive students completed radiography, among whom 62.50% had a Cobb angle ≥10°.

What are the implications for public health practice?

In resource-limited settings in northwestern China, priority referral and follow-up mechanisms targeting junior and senior high school students are needed to translate front-end screening into definitive evaluation and management.

ABSTRACT

Introduction: Scoliosis is a common spinal deformity affecting approximately 1.20% of school-age children in China. Amid the national scale-up of school-based spinal screening, evidence from multi-ethnic populations in northwestern China remains limited, and real-world data from Xinjiang Uygur Autonomous Region are lacking. This study reports AI-assisted and specialist-reviewed screening positivity rates in a multi-ethnic school population in Wusu City, northern Xinjiang.

Methods: This cross-sectional screening study was conducted in 16 schools in Wusu City, Xinjiang, in January 2026. Students aged 8–18 years underwent a three-stage pathway: 1) AI-assisted surface screening using a 3D electronic spine measuring instrument to acquire the angle of trunk inclination (ATI) during the Adams forward bend test (ATI ≥6° was defined as positive); 2) specialist clinical review to exclude postural scoliosis; 3) standing full-spine radiography for final screen-positive students (Cobb angle ≥10°). Screen-positive rates were compared across demographic and screening characteristics using chi-square tests and Cochran–Armitage trend tests.

Results: Among 22,479 registered students, 18,631 completed screening (82.88%). The AI-assisted screen-positive rate was 5.36% [95% confidence interval (*CI*): 5.05, 5.69], and the final screen-positive rate after specialist review was 2.62% (95% *CI*: 2.40, 2.86); both increased with age and school segment (trend *P*<0.001). Urban and Han students had higher positivity rates. AI-assisted screen positivity was higher in female students, whereas the sex difference in final screen positivity was not statistically significant. Only 24.59% of final screen-positive students completed radiography, among whom 62.50% had a Cobb angle ≥10°.

Conclusion: Junior and senior high school students should be prioritized in school-based scoliosis screening. In resource-limited settings, improving referral completion after an abnormal screen is as important as expanding screening coverage.

Scoliosis is a major public health concern among children and adolescents. Curve progression during periods of rapid growth may cause visible deformity,

Copyright © 2026 by Chinese Center for Disease Control and Prevention

pain, psychosocial distress, and functional impairment, imposing a substantial societal burden (*1*–*2*). School-based screening has therefore become increasingly common, consistent with the national "Five-Health" initiative for children and adolescents (*3*).

Recent studies have reported a pooled prevalence of adolescent scoliosis of approximately 1.20% in China (*4*). Despite extensive research, regional differences and possible demographic patterns remain incompletely characterized (*5*–*8*), and real-world screening evidence from multiethnic school populations in northwestern China, particularly in Xinjiang Uygur Autonomous Region, remains relatively scarce. Wusu City in northern Xinjiang, which has both Han and ethnic minority populations, provides a real-world setting for evaluating a school-based screening pathway in a resource-limited area but is not representative of the entire Xinjiang Uygur Autonomous Region.

Therefore, data from the Wusu City School Screening Program were analyzed to report the artificial intelligence (AI)-assisted and final screen-positive rates after specialist review, with the aim of informing targeted prevention and control strategies.

This cross-sectional screening study was conducted in January 2026 at 16 primary, junior high, and senior high schools in Wusu City, Xinjiang Uygur Autonomous Region, China. Participants were students aged 8–18 years. Students who had received previous treatment for spinal deformity; who had known congenital, neuromuscular, or syndromic spinal deformity; or who were absent or declined to participate on the screening day were excluded.

This screening pathway included three stages. In the first stage, AI-assisted surface screening, trained personnel used a three-dimensional (3D) electronic spine measuring instrument (MW01/MW02, Hunan Mawei Kang Cheng Technology Co., Ltd. Hunan, China; nominal angle accuracy ±1.00°) during the Adams forward bend test; the instrument scanned the body-surface contour from C7 to the lumbosacral region, and an embedded algorithm automatically acquired and recorded the angle of trunk inclination (ATI) in real time and provided an on-site AI grade. The AI algorithm was designed only for body-surface data acquisition, automated measurement, and on-site grading, and did not directly diagnose scoliosis; the radiographic Cobb angle remains the gold standard for confirmation. An ATI of ≥6° was defined as a positive AI screen, in accordance with the screening protocol of the 3D electronic spine measuring instrument used in this program; this cut-off lies within the 5°–7° angle-of-trunk-rotation range commonly used for scoliometer-based school screening and referral to radiography (*9*–*10*), and was adopted to reduce possible false-positive referrals from highly sensitive surface measurements while maintaining adequate sensitivity for clinically meaningful trunk asymmetry. This threshold is a screening criterion rather than a diagnostic standard.

In the second stage, specialist review, two spine specialists examined AI-positive students using postural inspection, palpation, and repeated forward bend tests, to assess shoulder asymmetry, scapular prominence, lumbar triangle asymmetry, pelvic obliquity, and paraspinal muscle tension (*9*–*10*). All specialists had received standardized training on the screening protocol, and ATI was remeasured with the same model of 3D electronic spine measuring instrument (MW01/MW02). Discrepancies were resolved by consensus discussion, and if consensus could not be reached, the more experienced specialist made the final determination. During the review, postural (non-structural) scoliosis arising from poor posture or transient positioning was excluded by correcting posture and re-testing after activity; only students with a fixed structural abnormality persisting on re-testing were defined as final screen positive and referred for imaging, whereas AI-positive students whose asymmetry resolved on re-testing were classified as marginal (borderline) cases and were not referred. In the third stage, hospital imaging, referred students underwent standing full-spine anteroposterior and lateral X-ray examination at the designated hospital, with a Cobb angle ≥10° taken as suggestive of scoliosis (*1*,*9*) (Figure 1). Cobb angles were measured by a single spine surgeon using standard digital radiography software, and a second reader independently re-measured 10% of the images for quality control.

Variables included sex, school segment, residential or school district (urban/rural), ethnicity (Han/minority), age group (<13/≥13 years), dietary pattern, and AI grade. AI grade was defined by ATI as grade 0 (<5°), grade 1a (5° to <6°), grade 1b (6° to <7°), grade 2 (7° to <10°), and grade 3 (≥10°). Dietary pattern (halal/non-halal) was used only as a crude sociocultural marker and was not interpreted as a direct nutritional exposure or a causal factor. The two primary outcomes were final screening positivity among all screened students and radiographic confirmation among those who underwent radiography in the primary analysis.

Continuous variables were summarized as means and standard deviations, and categorical variables were

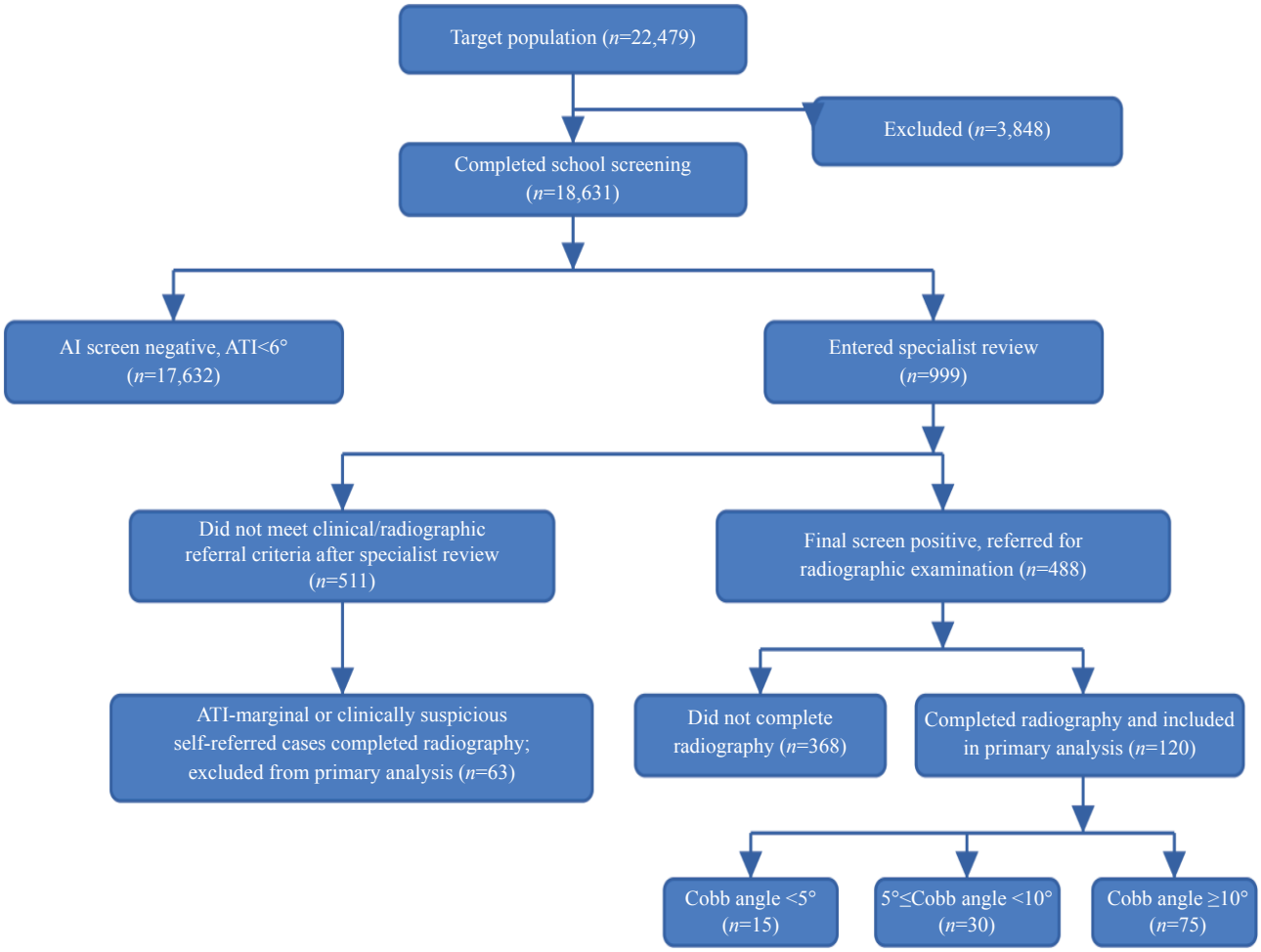

FIGURE 1. Scoliosis screening, specialist review, and radiographic confirmation pathway among students aged 8–18 years — Wusu City, Xinjiang Uygur Autonomous Region, China, January 2026.
Note: The 63 self-referred marginal cases were not included in the primary radiographic confirmation analysis.
Abbreviation: AI=artificial intelligence; ATI=angle of trunk inclination.

summarized as frequencies and percentages. AI-assisted and final screen-positive rates were calculated and stratified by sex, school segment, age group, urban/rural area, ethnicity, and AI grade, and subgroups were compared using Pearson chi-square tests, with Fisher's exact test when expected frequencies were small. Trends in screen-positive rates across the ordered variables — of age (in single years) and school segment (primary, junior high, senior high) — were assessed using the Cochran–Armitage trend test. All chi-square and trend tests were unadjusted (crude). Because age group was highly correlated with school segment, stratified analyses focused on age group, with school segment used descriptively. Statistical significance was set at $P<0.05$. Primary analyses were performed using IBM SPSS Statistics (version 26.0; IBM Corp., Armonk, NY, USA) and R (version 4.3.1; R Foundation for Statistical Computing, Vienna, Austria).

Among the 22,479 enrolled students, 18,631 (82.88%) completed screening. The 3,848 students (17.12%) who did not complete screening comprised those absent on the screening day (e.g., illness, personal leave, or off-campus activities), those whose parents declined participation, and a small number excluded for known spinal deformity or prior treatment; detailed reasons were not systematically recorded for every non-screened student. The mean age was 12.36 years, and female students accounted for 50.19% of the participants. Primary, junior high, and senior high school students accounted for 38.49%, 39.79%, and 21.72% of the participants, respectively. Han students represented 71.50% of the participants, and 90.75% were from urban schools or areas.

AI-assisted screening identified 999 positive students, with an AI positivity rate of 5.36% [95%

confidence interval (*CI*): 5.05, 5.69]. After specialist review, 488 students were classified as final screen positive, and the final screen-positive rate was 2.62% (95% *CI*: 2.40, 2.86) (Table 1). Among all screened students, 16,753 (89.92%) had an AI grade of 0, 879 (4.72%) grade 1a, 457 (2.45%) grade 1b, 419 (2.25%) grade 2, and 123 (0.66%) grade 3.

A total of 183 students completed imaging, including 120 referred from the final screen-positive group (24.59% of the 488) and 63 self-referred marginal cases that had been AI-positive but not classified as final screen positive after specialist review and therefore not formally referred; they presented for radiography on their own initiative. Among the 120 referred final screen-positive students who completed radiography, 75 (62.50% of these 120 students) had a Cobb angle ≥10°, 15 had a Cobb angle <5°, and 30 had a Cobb angle of 5° to <10°.

Among the 63 marginal (borderline) cases — not referred after specialist review but self-presenting for imaging— none had a Cobb angle ≥10°: 7 had a Cobb angle <5° and 56 had a Cobb angle of 5° to <10°. This pattern suggests that specialist review reduced false-positive referrals after front-end AI screening; however, these self-referred cases cannot be used to formally estimate sensitivity or specificity.

Screening abnormalities increased with age and school segment. AI positivity increased from 2.80% at 8 years of age to 10.28% at 16 years of age, and the final screening positivity increased from 1.07% to 5.68% (all *P* for trend <0.001, unadjusted). The final screen-positive rates in primary, junior high, and senior high school students were 1.37% (95% *CI*: 1.12, 1.66), 2.50% (95% *CI*: 2.16, 2.88), and 5.07% (95% *CI*: 4.43, 5.78), respectively (Figure 2).

Urban students had higher AI-assisted and final screen-positive rates than rural students [5.57% *vs.* 3.36%; 2.75% (95% *CI*: 2.51, 3.01) *vs.* 1.33% (95% *CI*: 0.89, 2.00)]. Han students had higher rates than minority students [AI 5.70% *vs.* 4.52%; final 2.80% (95% *CI*: 2.53, 3.09) *vs.* 2.17% (95% *CI*: 1.81, 2.59)]; these urban–rural and ethnic differences were statistically significant in unadjusted analyses. Female students had a slightly higher crude positivity than male students, but the difference in the final screen-positive rate by sex was not statistically significant

TABLE 1. Characteristics and scoliosis screening results among students aged 8–18 years — Wusu City, Xinjiang Uygur Autonomous Region, China, January 2026.

Characteristic	Screened students, *n*	AI-positive students, *n* (%)	Final screen-positive students, *n* (%)
Overall	18,631	999 (5.36)	488 (2.62)
Sex			
Male	9,281	462 (4.98)	222 (2.39)
Female	9,350	537 (5.74)	266 (2.84)
P		0.020	0.053
School segment			
Primary school	7,172	217 (3.03)	98 (1.37)
Junior high school	7,413	379 (5.11)	185 (2.50)
Senior high school	4,046	403 (9.96)	205 (5.07)
P for trend		<0.001	<0.001
Area			
Urban	16,907	941 (5.57)	465 (2.75)
Rural	1,724	58 (3.36)	23 (1.33)
P		<0.001	<0.001
Ethnicity			
Han	13,321	759 (5.70)	373 (2.80)
Minority	5,310	240 (4.52)	115 (2.17)
P		0.001	0.014

Note: AI-positive: ATI ≥6°. Final screen-positive: abnormal after specialist review and referred for radiography. *P* values from Pearson's chi-square test (sex, region, ethnicity) or Cochran–Armitage trend test (school segment). All analyses unadjusted. Percentages are row percentages.
Abbreviation: AI=artificial intelligence; ATI=angle of trunk inclination.

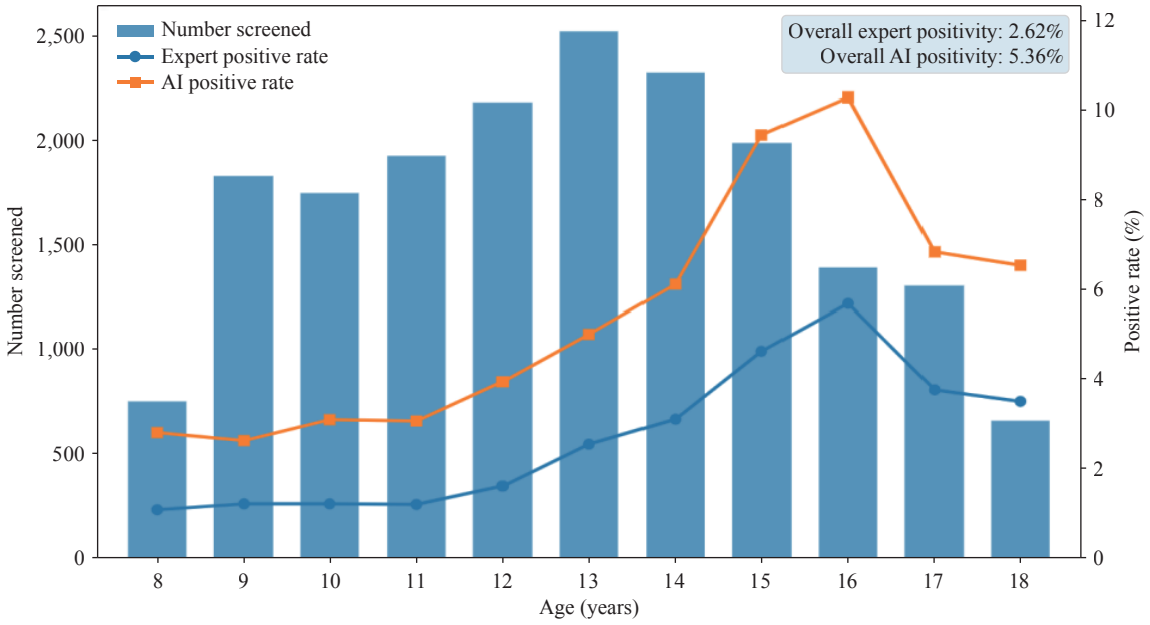

FIGURE 2. Age-specific numbers screened and scoliosis screen-positive rates among students aged 8–18 years — Wusu City, Xinjiang Uygur Autonomous Region, China, January 2026.
Note: Bars represent the number of screened students by age (left Y-axis). Lines represent age-specific positive rates (right Y-axis): AI-assisted (orange, squares) and final after specialist review (blue, circles). Both rates increased with age (*P* for trend <0.001), peaking at 15–16 years. The overall AI-assisted and final screen-positive rates were 5.36% and 2.62%, respectively.
Abbreviation: AI=artificial intelligence.

(*P*=0.053, unadjusted).

Of the 488 final screen-positive students, only 120 (24.59%) completed radiographic examination and 368 (75.41%) did not. As shown in Table 2, completers and non-completers differed significantly by age group (χ^2=7.99, *P*=0.005) and by urban/rural region (Fisher's exact test, P=0.013) in unadjusted analyses: students aged <13 years (31.67% *vs.* 19.29%) and rural students (9.17% *vs.* 3.26%) were more likely to complete imaging. No significant differences were observed by sex, school segment, ethnicity, dietary pattern, or AI grade (all *P*>0.05).

DISCUSSION

In this multiethnic school population in Wusu City, northern Xinjiang, AI-assisted screening identified 5.36% of students as screen-positive, decreasing to 2.62% after specialist review. This reduction suggests that specialist review excluded postural abnormalities and reduced false-positive referrals. AI-assisted screening therefore served as a triage rather than a diagnostic tool, with radiographic Cobb angle assessment used for confirmation. Because few screen-positive students completed radiography, population-level confirmed prevalence could not be estimated. The analysis therefore focused on AI-assisted and final screen-positive rates and their distribution across subgroups to inform school-based screening strategies in multiethnic areas.

Across this screening cascade, age was the most consistent factor associated with both AI-assisted and final screen-positive rates. Both rates increased markedly after 13 years of age and peaked at 15–16 years. This pattern is consistent with the pubertal growth spurt, during which spinal growth accelerates and vertebral biomechanics and neuromuscular control may become transiently imbalanced, potentially contributing to scoliosis onset or progression (*2*). These age-related findings may also inform screening strategies: when resources are limited, review, referral, and follow-up could prioritize students aged ≥13 years, especially those in junior and senior high schools (*2*,*9*).

Urban and Han students had higher screen-positive rates than their rural and minority counterparts. However, these differences more likely reflect the composition of the screened population, school distribution, and healthcare-seeking behavior rather than true etiological variation (*5*–*8*); the binary Han/minority classification also simplifies the region's multi-ethnic diversity (*6*). Subgroup differences should therefore be viewed as clues for identifying high-

TABLE 2. Characteristics of final screen-positive students by X-ray completion status — Wusu City, Xinjiang Uygur Autonomous Region, China, January 2026.

Variable	Completed X-ray (*n*=120), *n* (%)	Not completed (*n*=368), *n* (%)	χ^2	*P*
Sex			3.29	0.070
Male	46 (38.33)	176 (47.83)		
Female	74 (61.67)	192 (52.17)		
School segment			4.05	0.132
Primary	28 (23.33)	70 (19.02)		
Junior high	51 (42.50)	134 (36.41)		
Senior high	41 (34.17)	164 (44.57)		
Ethnicity			0.10	0.751
Han	93 (77.50)	280 (76.09)		
Minority	27 (22.50)	88 (23.91)		
Region			–	0.013*
Rural	11 (9.17)	12 (3.26)		
Urban	109 (90.83)	356 (96.74)		
Dietary pattern			0.04	0.834
Halal	25 (20.83)	80 (21.74)		
Non-halal	95 (79.17)	288 (78.26)		
Age group			7.99	0.005
<13 years	38 (31.67)	71 (19.29)		
≥13 years	82 (68.33)	297 (80.71)		
AI grade			0.46	0.793
Grade 1b	31 (25.83)	104 (28.26)		
Grade 2	65 (54.17)	199 (54.08)		
Grade 3	24 (20.00)	65 (17.66)		

Note: *P* values from Pearson's chi-square test except region. "–" denotes "not applicable"; no χ^2 statistic is reported because Fisher's exact test was used. All analyses unadjusted. Percentages are column percentages. AI grade 1b = ATI 6° to <7°; grade 2 = ATI 7° to <10°; grade 3 = ATI ≥10°.
Abbreviation: AI=artificial intelligence; ATI=angle of trunk inclination.
* Fisher's exact test.

priority groups for follow-up rather than as evidence of causal risk factors.

These findings further point to a key implementation challenge: incomplete radiographic follow-up. Only 120 (24.59%) of final screen-positive students completed radiography, whereas 368 (75.41%) did not, limiting the transition from initial screening to definitive imaging evaluation and subsequent management (*9*–*10*). Reasons for non-completion may include parental concern about children's exposure to ionizing radiation (*11*); the costs, time, and travel required for hospital-based radiography; and limited awareness of scoliosis and consequent low prioritization. These factors were not systematically collected in this study. Because completers were disproportionately younger and from rural areas (Table 2), the 75 imaging-confirmed cases may not be representative of all final screen-positive students. Therefore, the 62.50% with a Cobb angle ≥10° among those who completed radiography should not be extrapolated to all 488 final screen-positive students or used to estimate population-level prevalence.

This study has two main limitations. First, the low radiographic follow-up rate precluded estimation of population-level confirmed prevalence, a common constraint in school screening programs driven by parental concern about radiation and healthcare accessibility. Second, inter-observer agreement for specialist review and Cobb angle measurement was not formally assessed, and non-completion of screening may introduce selection bias, although the completion rate compares favorably with similar programs. Despite these limitations, this study provides real-world data on a multi-ethnic school screening pathway in

northwestern China and indicates that improving referral completion is central to realizing the benefits of screening. In resource-limited settings, raising parental awareness of scoliosis and the importance of post-screening follow-up is essential to improving referral completion. Age-stratified screening strategies should prioritize junior and senior high school students (aged ≥13 years), the highest-risk group. Establishing targeted follow-up mechanisms for key populations offers a practical pathway for implementing the national "Five Health Priorities" spinal screening campaign.

Conflicts of interest: No conflicts of interest.

Ethical statement: Approved by the Scientific Research Ethics Committee of Shanghai University of Sport (approval no. 102772024RT100). Written informed consent was obtained from the participants' parents or legal guardians.

Funding: Supported by the National Key Research and Development Program of China project "Establishment of a Precision Diagnosis and Treatment System and Development of Key Technologies for Neural Tube Defects Across the Entire Disease Course Based on Functional Preservation and Reconstruction": Development of a Precision Diagnosis and Treatment System for Neural Tube Defects and Key Technologies (Clinical Research Type) (Grant Number 2025YFC2511500) and the National Natural Science Foundation of China project "The Role and Mechanism of RUNX1-Mediated Ferroptosis in Paravertebral Muscle Fibro/Adipogenic Progenitor Cells (FAPs) in the Pathogenesis of Adolescent Idiopathic Scoliosis" (Grant Number 82572701).

doi: 10.46234/ccdcw2026.190

[#] Corresponding authors: Xinfeng Zheng, zhengxinfeng@xinhuamed.com.cn; Xiaofeng Peng, pengxiaofeng11@163.com.

[1] Spine Center, Xinhua Hospital Affiliated to Shanghai Jiao Tong University School of Medicine, Shanghai, China; [2] The Second Clinical Medical College, Zhejiang Chinese Medical University, Hangzhou City, Zhejiang Province, China; [3] Department of Spinal Surgery, The First Affiliated Hospital of Xinjiang Medical University, Urumqi City, Xinjiang Uygur Autonomous Region, China; [4] Institute of Reproductive and Child Health / National Health Commission Key Laboratory of Reproductive Health, Peking University, Beijing, China; [5] Department of Epidemiology and Biostatistics, School of Public Health, Peking University, Beijing, China; [6] School of Exercise and Health, Shanghai University of Sport, Shanghai, China; [7] Department of Orthopedics, Wusu People's Hospital, Wusu City, Xinjiang Uygur Autonomous Region, China.

[&] Joint first authors.

Copyright © 2026 by Chinese Center for Disease Control and Prevention & Chinese Academy of Preventive Medicine. All content is distributed under a Creative Commons Attribution Non Commercial License 4.0 (CC BY-NC).

Submitted: May 12, 2026
Accepted: September 10, 2026
Issued: September 18, 2026

REFERENCES

1. Weinstein SL, Dolan LA, Cheng JC, Danielsson A, Morcuende JA. Adolescent idiopathic scoliosis. Lancet 2008;371(9623):1527 – 37. https://doi.org/10.1016/S0140-6736(08)60658-3.
2. Dimeglio A, Canavese F. Progression or not progression? How to deal with adolescent idiopathic scoliosis during puberty. J Child Orthop 2013;7(1):43 – 9. https://doi.org/10.1007/s11832-012-0463-6.
3. National Health Commission of the People's Republic of China, National Administration of Disease Control and Prevention, Office of the Central Cyberspace Affairs Commission, National Development and Reform Commission, Ministry of Education of the People's Republic of China, Ministry of Finance of the People's Republic of China, et al. Notice on issuing the action plan for promoting the "five-health priorities" among children and adolescents (2026-2030). 2025. https://www.nhc.gov.cn/fys/c100078/202512/9c3da4badfb34026b5fabbf5853105ee.shtml. [2026-3-25]. (In Chinese).
4. Fu XL, Meng SL, Huang XT, Li W, Ye BS, Chen SW. The prevalence of scoliosis among adolescents in China: a systematic review and meta-analysis. J Orthop Surg Res 2024;19(1):585. https://doi.org/10.1186/s13018-024-05077-0.
5. Xu S, Li KX, Jin LY, Dong YH, Liang Y, Liu CJ, et al. Distribution of scoliosis in 2.22 million adolescents in mainland China: a population-wide analysis. J Glob Health 2024;14:04117. https://doi.org/10.7189/jogh.14.04117.
6. Hu CX, Lin BC, Li FT, Li ZX, Chen XZ. Prevalence and associated factors of multi-ethnic adolescent idiopathic scoliosis in Longlin, Southwestern China: a school-based cross-sectional study. Front Public Health 2025;13:1729509. https://doi.org/10.3389/fpubh.2025.1729509.
7. Huang J, Zhang HT, Wen JT, Liu LL, Xu SH, Wang XS, et al. Evaluation of the prevalence of adolescent scoliosis and its associated factors in Gansu Province, China: a cross-sectional study. Front Public Health 2024;12:1381773. https://doi.org/10.3389/fpubh.2024.1381773.
8. Tu QY, Xu WB, Feng YQ, Zhang ZW, Zhuang W. Prevalence and determinants of adolescent idiopathic scoliosis from school screening in Xiaoshan District, Hangzhou, China. Front Public Health 2025;13:1595793. https://doi.org/10.3389/fpubh.2025.1595793.
9. Zhao Y, Zhao Y, Lu S, Yang Q, Chen L, Ma XL, et al. Guideline for adolescent scoliosis screening in China (public version 2024). J Orthop Translat 2025;50:364 – 72. https://doi.org/10.1016/j.jot.2024.09.006.
10. Dunn J, Henrikson NB, Morrison CC, Blasi PR, Nguyen M, Lin JS. Screening for adolescent idiopathic scoliosis: an evidence report and systematic review for the US Preventive Services Task Force. JAMA 2018;319(2):173 – 87. https://doi.org/10.1001/jama.2017.11669.
11. Luan FJ, Wan Y, Mak KC, Ma CJ, Wang HQ. Cancer and mortality risks of patients with scoliosis from radiation exposure: a systematic review and meta-analysis. Eur Spine J 2020;29(12):3123 – 34. https://doi.org/10.1007/s00586-020-06573-7.

Youth Editorial Board

Director Lei Zhou

Vice Directors Jue Liu Tiantian Li Tianmu Chen

Members of Youth Editorial Board

Jingwen Ai
Liangliang Cui
Jia Huang
Min Kang
Fangfang Li
Jun Liu
Yang Pan
Shuhui Song
Jingyuan Wang
Xin Wang
Meng Xiao
Lin Yang
Yang Zhao
Li Bai
Meng Gao
Xiang Huo
Huihui Kong
Jingxin Li
Li Liu
Zhixing Peng
Kun Su
Linghang Wang
Feixue Wei
Tian Xiao
Canqing Yu
Hong Zhou
Yuhai Bi
Jie Gong
Xiaolin Jiang
Lingcai Kong
Huigang Liang
Yang Liu
Menbao Qian
Song Tang
Qihui Wang
Yongyue Wei
Wuxiang Xie
Lin Zeng
Yunlong Cao
Yuehua Hu
Yu Ju
Shengjie Lai
Di Liu
Chao Ma
Tian Qin
Bin Wang
Xiaoli Wang
Zhiqiang Wu
Lei Xu
Yi Zhang

Indexed by Science Citation Index Expanded (SCIE), Social Sciences Citation Index (SSCI), PubMed Central (PMC), Scopus, Chinese Scientific and Technical Papers and Citations, and Chinese Science Citation Database (CSCD)

Copyright © 2026 by Chinese Center for Disease Control and Prevention & Chinese Academy of Preventive Medicine

Under the terms of the Creative Commons Attribution-Non Commercial License 4.0 (CC BY-NC), it is permissible to download, share, remix, transform, and build upon the work provided it is properly cited. The work cannot be used commercially without permission from the journal.

References to non-China-CDC sites on the Internet are provided as a service to *CCDC Weekly* readers and do not constitute or imply endorsement of these organizations or their programs by China CDC or National Health Commission of the People's Republic of China. China CDC is not responsible for the content of non-China-CDC sites.

The inauguration of *China CDC Weekly* is in part supported by Project for Enhancing International Impact of China STM Journals Category D (PIIJ2-D-04-(2018)) of China Association for Science and Technology (CAST).

CHINA CDC WEEKLY

CCDC weekly

Vol. 8 No. 38 Sept. 18, 2026

中国疾病预防控制中心周报(英文)

Responsible Authority
National Disease Control and Prevention Administration

Sponsor
Chinese Center for Disease Control and Prevention &
Chinese Academy of Preventive Medicine

Editor-in-Chief
Jianwei Wang

Editing and Publishing
China CDC Weekly Editorial Office
No.155 Changbai Road, Changping District, Beijing, China
Tel: 86-10-63150501, 63150701
Email: weekly@chinacdc.cn

Printing: Beijing Kexin Printing Co., Ltd

Complimentary Access

CSSN
ISSN 2096-7071 (Print)
ISSN 2097-3101 (Online)
CN 10-1629/R1